Remote sensing of atmospheric aerosols and trace gases by means of Multi-Filter Rotating Shadowband Radiometer. Part II: Climatological applications

Mikhail D. Alexandrov
Department of Applied Physics, Columbia University and NASA Goddard Institute for Space Studies, New York

Andrew A. Lacis, Barbara E. Carlson
NASA Goddard Institute for Space Studies, New York

Brian Cairns
Department of Applied Physics, Columbia University and NASA Goddard Institute for Space Studies, New York

Abstract

Measurements from ground-based sunphotometer networks can be used both to provide ground-truth validation of satellite aerosol retrievals and to produce a land-based aerosol climatology that is complementary to satellite retrievals that are currently performed mostly over ocean. The Multi-Filter Rotating Shadow-band Radiometer (MFRSR) has become a popular network instrument in recent years. Several networks operate about a hundred instruments providing good geographical coverage of the United States. In addition, international use of the MFRSR has continued to increase, allowing MFRSR measurements to significantly contribute to aerosol climatologies.

In this study we investigate the feasibility of creating a ground-based aerosol climatology using MFRSR measurements. Additionally, this analysis allows us to test the performance of our retrieval algorithm under a variety of conditions. We use our retrieval algorithm for processing MFRSR data from clear and partially cloudy days to simultaneously retrieve daily time series of column mean aerosol particle size, aerosol optical depth, NO_2, and ozone column amounts together with the instrument's calibration constants directly from the MFRSR measurements for a variety of sites covering a range of atmospheric and surface conditions. This analysis provides a description of seasonal changes in aerosol parameters and in column amounts of ozone and NO_2 as a function of geographical location. In addition, we investigate the relationship between NO_2 column amount and aerosol optical depth as a potential indicator of tropospheric pollution. Application of this analysis method to the measurements from growing numbers of MFRSRs will allow us to expand on this developing climatology.

1. Introduction

Tropospheric aerosols with their direct and indirect radiative forcing continue to be one of the most significant sources of uncertainty in climate change modeling. While the retrieval of the spatial and temporal distribution of aerosol on a global scale is a task for satellite measurements (such as AVHRR, TOMS, MODIS, MISR), the increased emphasis on satellite aerosol retrievals has created the need for accurate ground-based, ground-truth aerosol measurements with which to validate satellite aerosol retrievals over land. In addition, measurements from ground-based sunphotometer networks can also be also used to produce a land-based aerosol climatology that is complementary to the satellite retrievals.

The Multi-Filter Rotating Shadow-band Radiometer (MFRSR) (Harrison et al. 1994) has become a popular instrument in recent years. Several existing networks operate about a hundred instruments providing good geographical coverage within the US. The list of MFRSR users includes Solar Irradiance Research Network (SIRN, http://sunphoto.giss.nasa.gov) sponsored by NASA, DOE ARM Southern Great Plains Site (http://www.arm.gov/docs/sites/sgp), ASRC sunphotometer network (http://hog.asrc.cestm.albany.edu/ rsr), and USDA UVB Radiation Monitoring Program (Bigelow et al. 1998, http://uvb.nrel.colostate.edu)). There is also a growing number of independent research groups that utilize the MFRSR.

The MFRSR makes simultaneous measurements of the direct solar beam extinction, and horizontal diffuse flux, at six wavelengths (nominally 415, 500, 615, 670, 870, and 940 nm) at one minute intervals throughout the day. The gaseous absorbers within the MFRSR channels are NO_2 (at 415, 500, and 615 nm) and ozone (at 500, 615, and 670 nm) and water vapor at 940 nm. Aerosols and Rayleigh scattering contribute atmospheric extinction in all MFRSR channels.

If the instrument calibration is accurately known and the unique spectral signature of each atmospheric constituent is available, retrievals can be obtained from the direct beam measurements to provide the daily time series of aerosol, NO_2, ozone and water vapor variability. In practical applications, laboratory and field calibration procedures using standard lamps are not able to provide calibrations of sufficient accuracy (cf. calibration-related references in the companion paper (Alexandrov et al. 2001)). There-

fore, a number of techniques have been developed to derive the calibration directly from the measurements. Traditionally, instrument calibration has been obtained using the Langley method at high altitude sites. While this approach can yield accurate calibrations when it can be implemented it is not well suited for network applications since changes in calibration can occur between successive high-altitude Langley calibrations.

Most MFRSR sites are not high altitude sites. Nevertheless, all of our sites have some days that are suitable for Langley calibration but the quality of the Langley calibration varies between sites depending on the stability of the atmosphere. To compensate for these variations in atmospheric stability, improved calibration can be obtained by averaging Langley-derived calibration coefficients over 20-40 clear days (Harrison and Michalsky 1994). Unfortunately, even this technique is not applicable to all sites. For example, there are urban locations where the aerosol optical depth may change throughout the day in response to anthropogenic sources, and there are places with frequent cloud cover with long periods of time between days that are suitable for Langley calibrations. Thus, a different calibration approach is required.

To improve this situation, we developed a new calibration/retrieval method for processing of MFRSR data from clear and partially cloudy days (Alexandrov et al. 1997, 1999b, 1999c, 2001) which has two advantages when compared with the Langley calibration technique. First, use of the direct to diffuse ratio in our regression method increases the stability of the regression and decreases the noise in the retrieved calibration coefficients when compared to the Langley technique. Second, since this method has different sensitivities to atmospheric stability we are able to use it on data for which Langley regression fails. Thus, we are able to include more data in the determination of the calibration coefficients.

In this paper, we briefly review the main features of our retrieval algorithm (cf. Alexandrov et al. 2001 for the details) and then present sample results of our retrievals and discuss their potential value for climate studies. Our approach is different from the methods frequently used in MFRSR data analysis. Instead of using correlative measurements for gas column amounts, we obtain a self-consistent retrieval of the column amounts of the gaseous absorbers as well as the aerosol properties. Due to the spectral trade-offs between NO_2 absorption and small particle extinction (parameterized here in terms of the variance
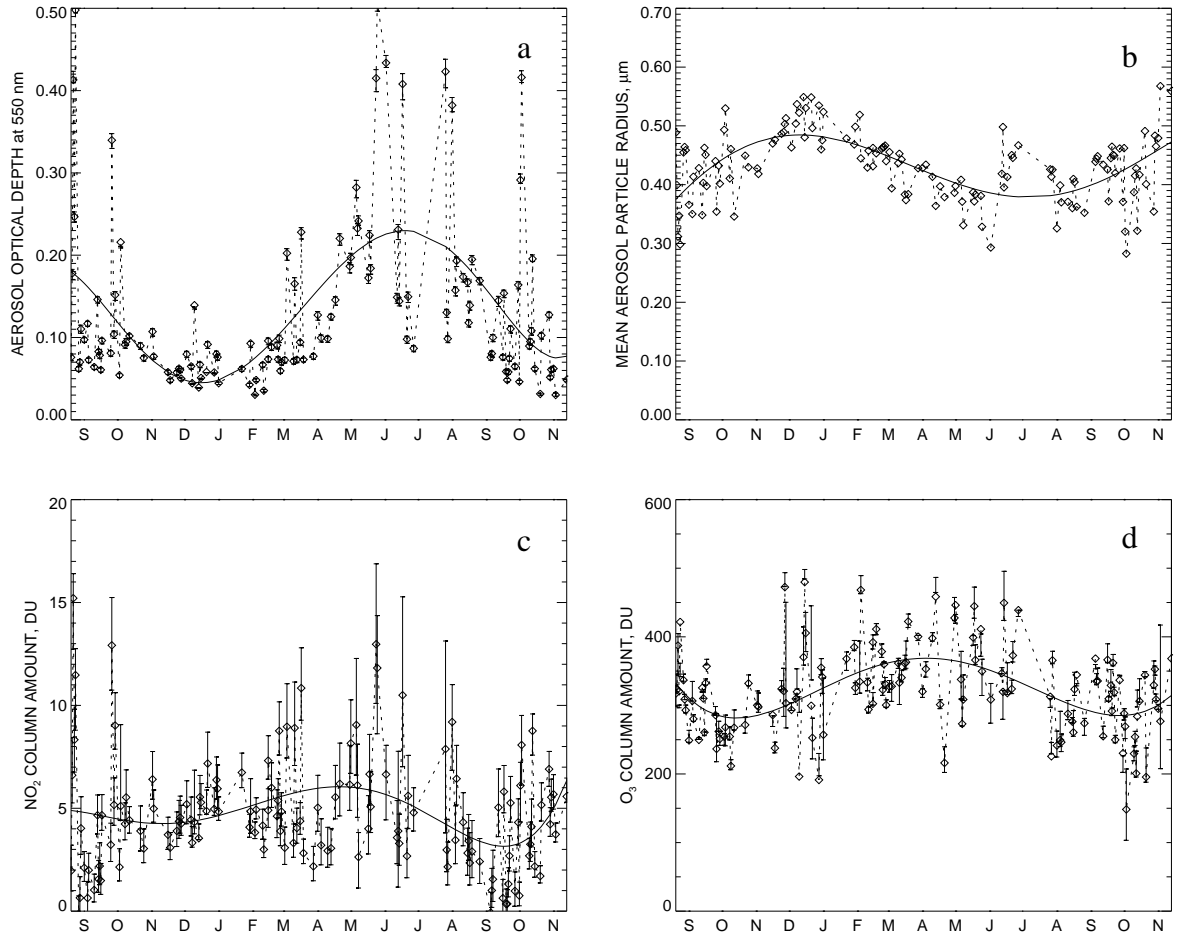
Figure 1.: Seasonal behavior of aerosol optical depth at 550 nm (a), mean column radius of the aerosol particles (b), NO_2 (c) and ozone (d) column amounts for New York City site, September 1995 – November 1996. Error bars show the uncertainties due to similarity of the spectral shapes of NO_2 absorption and aerosol extinction. Smooth solid curves represent polynomial fit to the data. The retrievals are made using instantaneous daily calibrations.
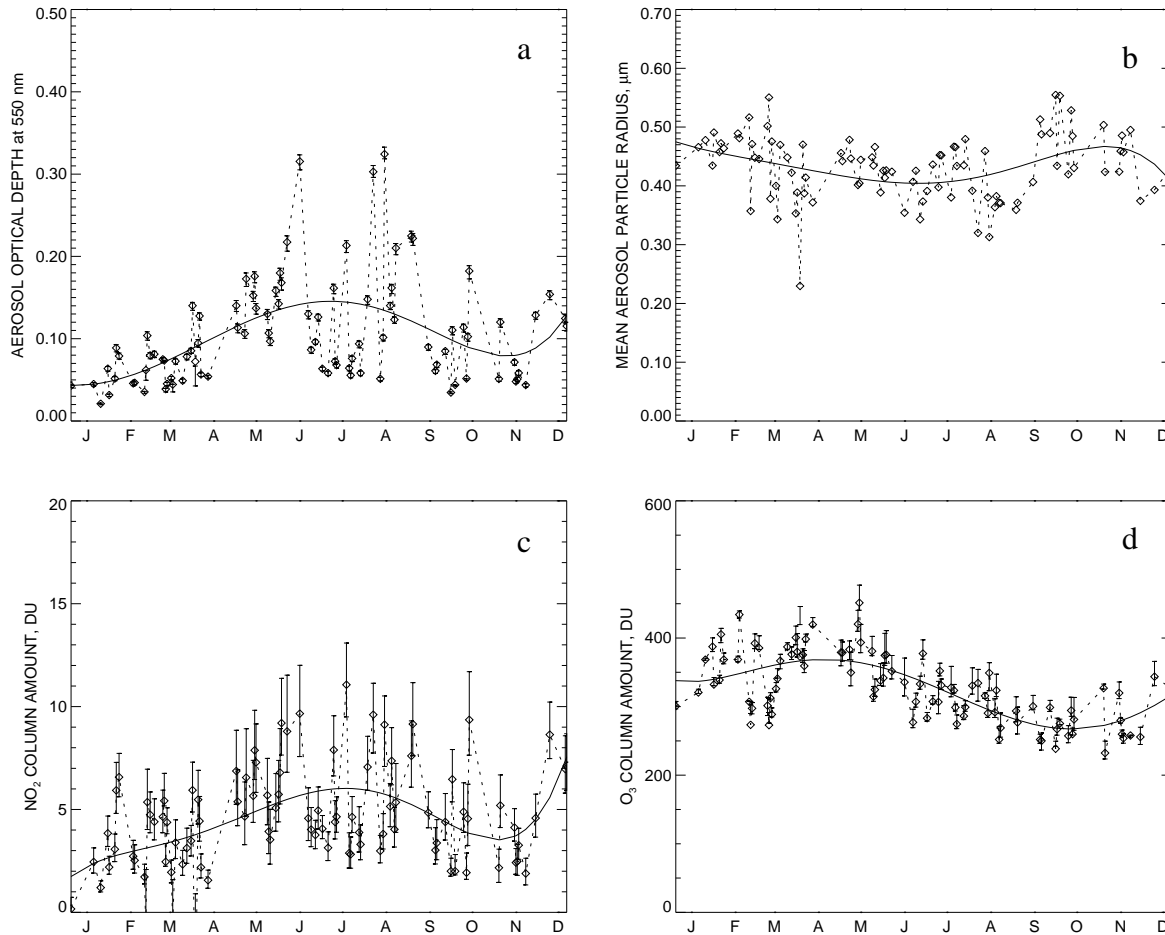
Figure 2.: Same as Fig. 1 but for Albany, New York, January – December, 1996.

of the aerosol size distribution), we use a range of variances to characterize the uncertainty in our retrieved products that is introduced by our inability to uniquely constrain the width of the aerosol size distribution. Nonetheless, our results and the relationship at some sites between aerosol optical depth and column NO_2 amount, are sufficiently robust to conclude that tropospheric NO_2 is highly variable and should be included in aerosol retrievals.

2. Method overview

The primary difference between our method and more traditional approaches to MFRSR data analysis is that we do not separate the calibration and retrieval procedures. Traditionally retrievals are made

from the data after the instrument's calibration constants have been determined (through a calibration procedure) and applied to the data. In our approach, we first separate contributions of different physical parameters (such as aerosol extinction, gaseous absorption) into total optical depths, and then calibrate them independently. Thus calibration errors in one parameter do not affect the accuracy of the other retrievals.

The first step in our method uses consistency between direct normal measurements and the direct to diffuse ratios in the 870 nm channel (the only channel not affected by gaseous absorption) to determine (aerosol) optical depth and the calibration constant for this channel. The direct to diffuse ratios are
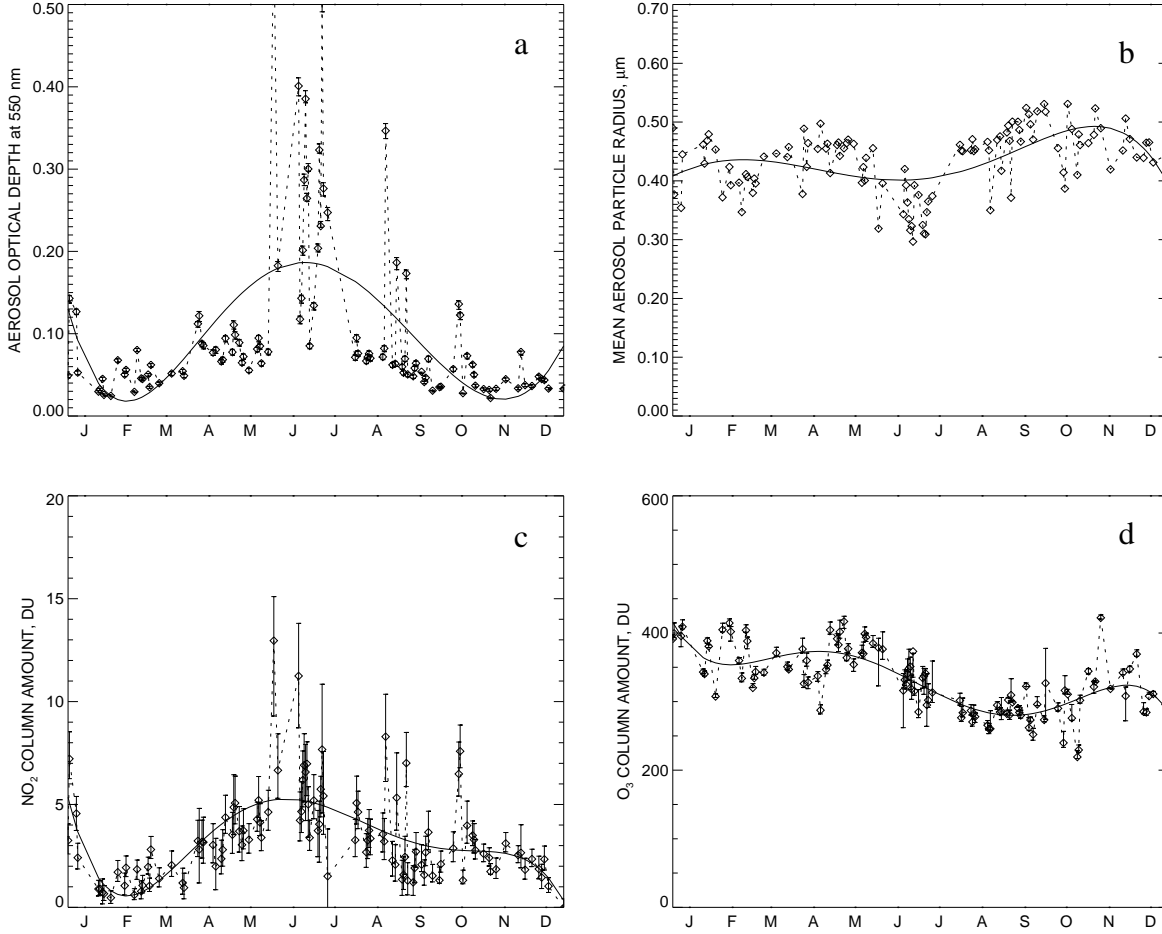
Figure 3.: Same as Fig. 1 but for Howland, Maine, January – December, 1995.

calibration independent sources of information (since for the MFRSR both direct and diffuse intensities are measured by the same detector). They can be used for example to determine the surface albedo and the aerosol absorption index (Herman et al. 1975) provided that the instrument is calibrated by other means, or they can be used to determine the aerosol optical depth under certain assumptions of aerosol absorption and surface albedo (O'Neill et al. 1989) (laboratory or Langley calibration is unnecessary in this case). The optical depth determined in this manner is less accurate than that obtained from direct measurements, so we use comparison between the two to determine the instrument's calibration, and then use it to correct the "direct" optical depth.

Inversion of aerosol optical depth, AOD, from the direct to diffuse ratios requires modeling the diffuse flux. To do this we performed multiple scattering calculations using the doubling and adding method with a Henyey-Greenstein phase function (Hansen and Travis 1974). Sensitivity studies have shown that the retrieved optical depth does not depend on the details of the phase function used since calculations using a full Mie phase function yield nearly identical results. Moreover, for any reasonable assumption of the surface albedo (e.g., $0 < A < 50\%$) this approach yields the optical depth (or, equivalently, the calibration coefficient in 870 nm channel), with an accuracy better than ± 0.01 (Alexandrov et al. 1999c).
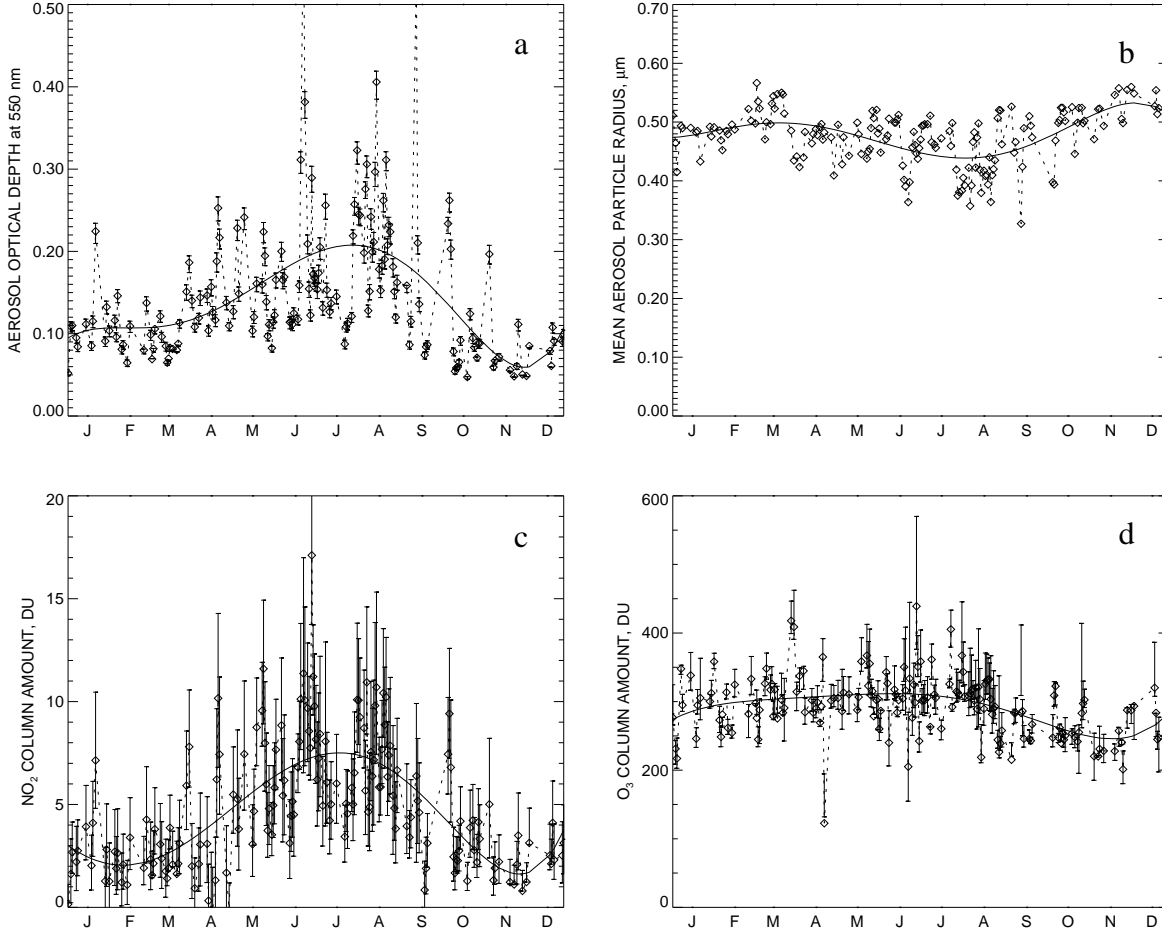
Our method has some limitations. For example,

Figure 4.: Same as Fig. 1 but for Southern Great Plains, Oklahoma, January – December, 1994.

it cannot be used when broken clouds outside the field of view of the direct beam measurements scatter photons into the diffuse beam. This multiply scattered radiation from the side is not accounted for in our plane-parallel "clear-sky" radiative model. However, since this multiply scattered light only affects the diffuse beam measurements, we can fall back on either our direct-beam analysis method (Lacis et al. 1996), use the Langley technique to determine the calibration coefficient for the 870 nm channel data, or transfer the calibration from a clearer day. (This suggests that inconsistencies between the direct and diffuse measurements can be used to examine 3D radiative effects and to determine cloud heterogeneity statistics.)

After the aerosol optical depth in the 870 nm channel has been determined, a regression technique is used to retrieve daily time series of column mean aerosol particle size (we present values of the "monodistribution radius", defined in (Alexandrov et al. 2001), aerosol optical depth in all channels, NO_2 and ozone column amounts together with the calibration coefficients for the first four channels. This technique uses regressions that are similar to Langleys. However, instead of total optical depth stability, they rely on the substantially better stabilities of the spectral shape of aerosol extinction and gas column amounts.

We have validated our retrieval algorithm by comparing our calibration coefficients and optical depths for an exceptionally clear data set from Davis, Califor-
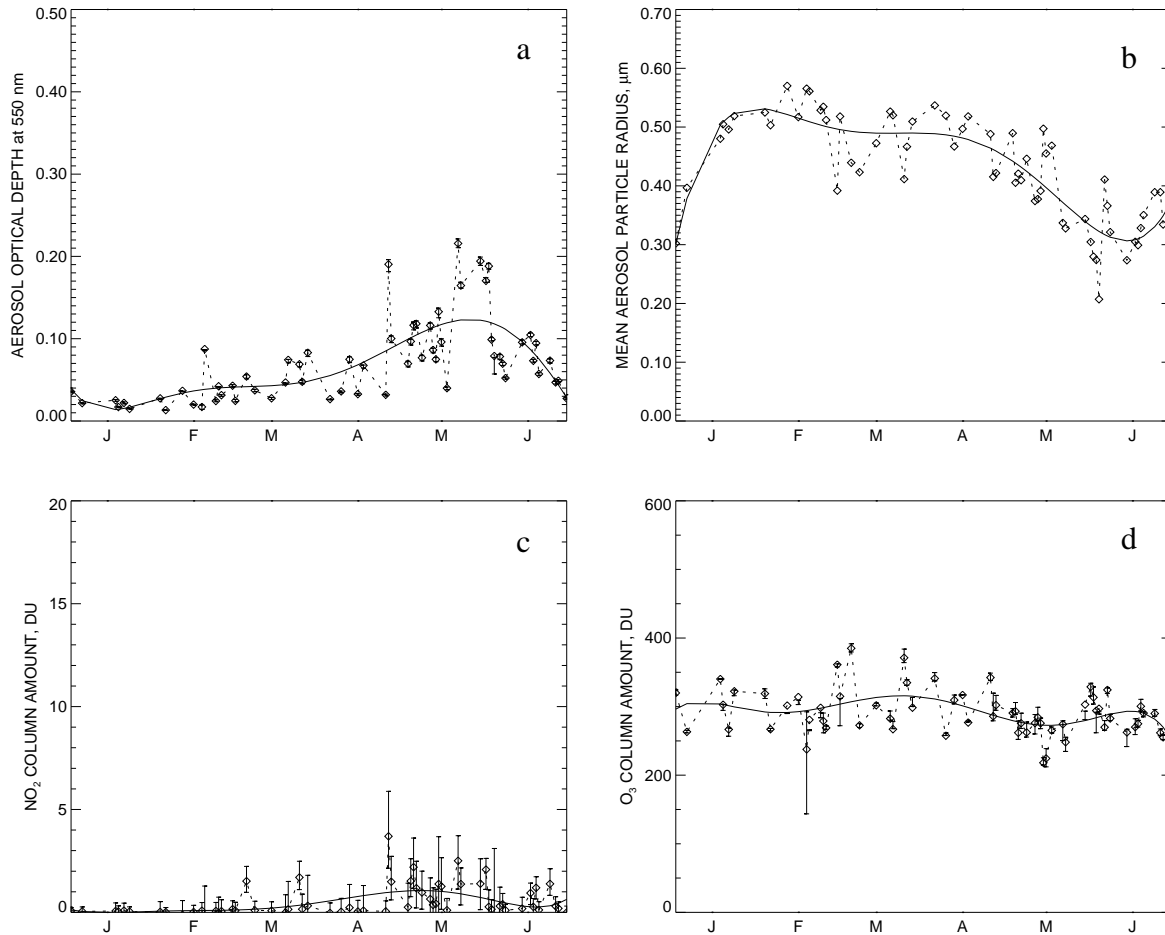
Figure 5.: Same as Fig. 1 but for the Central Plains Experimental Range, Colorado, January – June, 1996.

nia with those derived using the traditional Langley approach. As another check on our analysis method, we compared our retrieved aerosol optical depths with those derived from a co-located CIMEL sun/sky radiometer that is part of the AERONET (Holben et al. 1999) and found agreement to be better than 0.01. We also compared our ozone column amounts with those retrieved by TOMS as well as from nearby Brewer spectrometers. We find generally good agreement with a bias and standard deviation that depends on the location with some indication that MFRSR instrumental effects may contribute to these differences. Validation of our NO_2 column amounts is complicated by the paucity of tropospheric NO_2 measurements. While our retrieved column amounts

are smaller than the GOME tropospheric residuals, they are in agreement with column amounts retrieved from ground-based differential absorption spectrometers (e.g., Schroeder and Davies 1987). Retrieving NO_2 column amount from differential spectral measurements in the MFRSR spectral range is complicated by the similarity in the spectral gradient of NO_2 absorption and small particle aerosol extinction (Shaw 1976). In this respect, our retrieval is not fully unique in that it is possible to trade total extinction between NO_2 absorption and small particle extinction. This produces a family of solutions bracketed by the extremes in the variance of the size distribution which results in a greater uncertainty in the retrieved NO_2 column amount (about 30-50%).
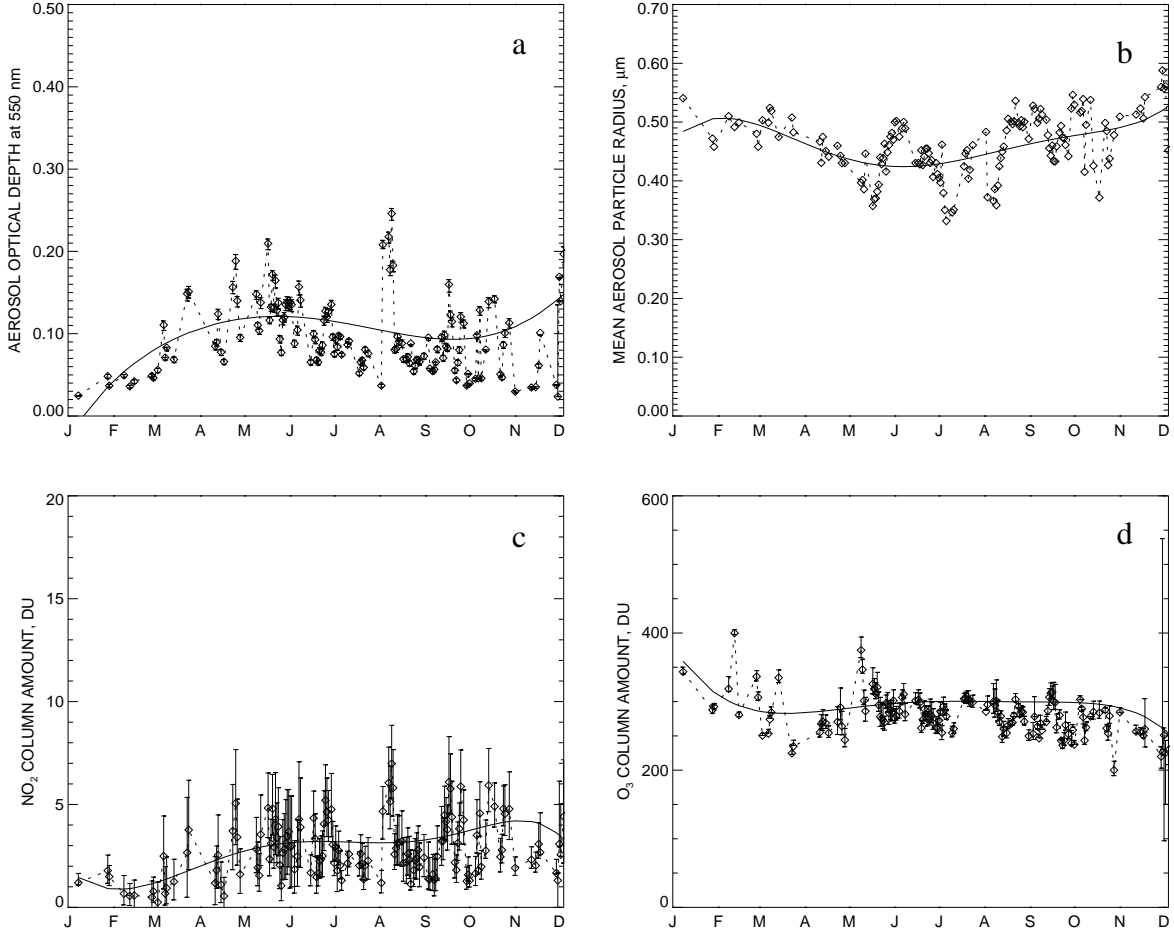
Figure 6.: Same as Fig. 1 but for Davis, California, January – December, 1996.

3. Results

We have used our algorithm to analyze MFRSR measurements from a number of instruments including those operated by large networks and those operated by individual investigators. To date, we have processed only a small fraction of the available MFRSR data with the primary goal of testing our retrieval algorithm under various geographical and climatological conditions. We present the results of our analysis from our test sites which include nine sites in the continental U.S. and from the islands (Mauna Loa, Hawaii, Bermuda and Barbados). For each site, we have analyzed at least a year of data and at many of these sites several years of data. Upon completing our testing, we will analyze a larger portion of the MFRSR data to substantially increase the temporal and geographic coverage of our retrieval results.

The analysis of long-term MFRSR measurements provides a description of seasonal and inter-annual changes in aerosol optical depth and particle size, as well as column amounts of ozone, NO_2 and water vapor as a function of geographical location (Alexandrov et al. 2000). This information can be used for comparison with both transport models and satellite measurements.

Our retrievals show that in most places aerosol properties exhibit pronounced seasonal changes with the magnitude dependent on geographical location which reflects the local atmospheric processes that lead to the formation, transport and deposition of
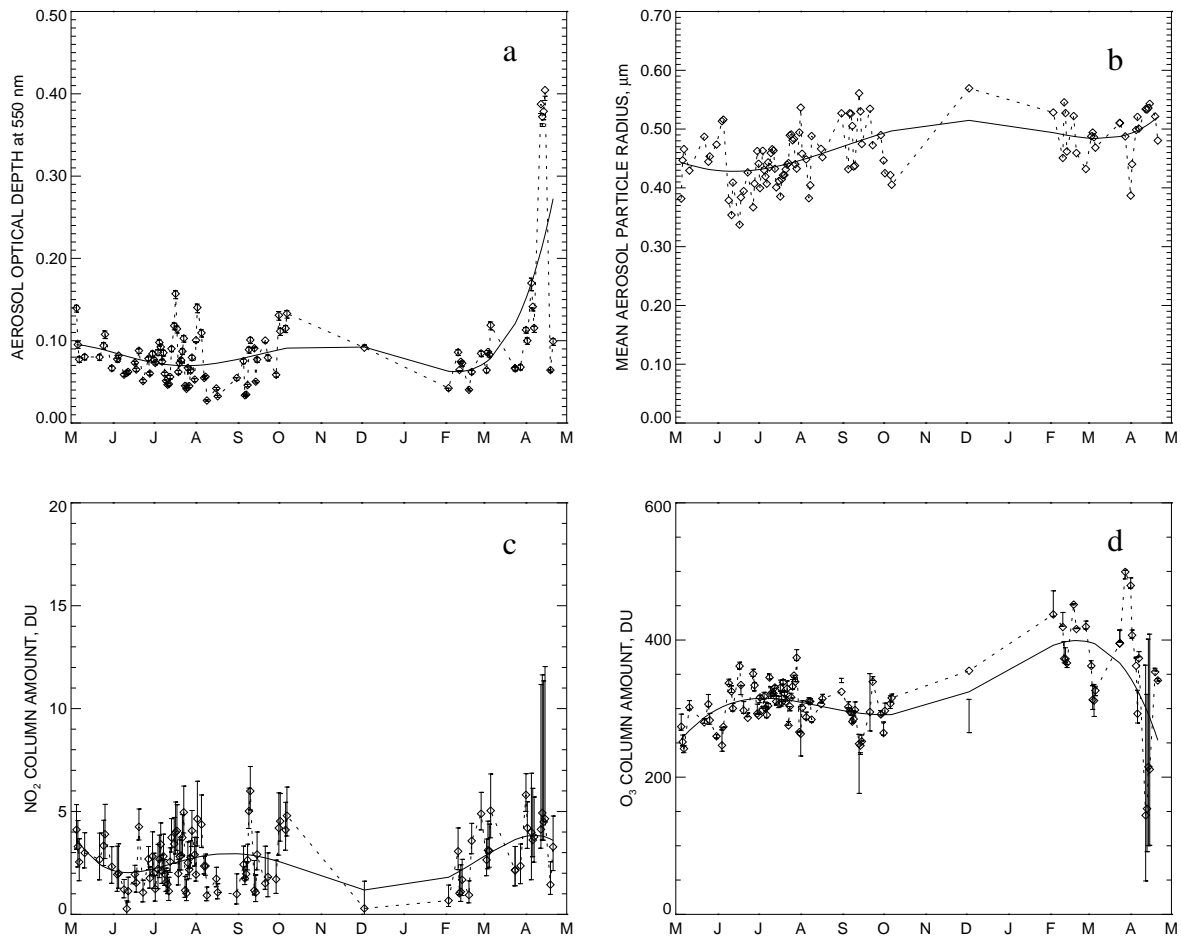
Figure 7.: Same as Fig. 1 but for Eugene, Oregon, May, 1997 − May, 1998.

aerosols and trace gases. As an illustration, we present in Figs. 1− 7 plots of time series of daily mean retrievals from sites representing the Western, Central and Eastern portions of the U.S. (Note that the time periods may be different for each site). Ozone and NO_2 column values are given in Dobson units (1DU = 2.687 ×$10^{16} mol/cm^2$). The error bars in these plots depict uncertainties due to trade-offs between NO_2 absorption and small particle aerosol extinction. In these figures, the smooth solid curves are polynomial fits to the data. The retrievals presented use smoothed calibration coefficients and are made using the algorithm described in detail in Alexandrov et al. (2001).

According to global aerosol transport modeling re-

sults (e.g., Tegen et al. 1997), sulfates dominate the contribution to the aerosol optical thickness in the Eastern US, while on the West Coast soil and sea salt aerosols also contribute. These aerosol model results are in agreement with data from the IM-PROVE sampling network (Malm and Sisler 2000). However, the IMPROVE data also indicates that pollution-generated nitrates contribute to the fine mode aerosols in Southern California (they are significant in Northern California as well). Organic carbon aerosols constitute the main part of the fine aerosol mass in Pacific North West.
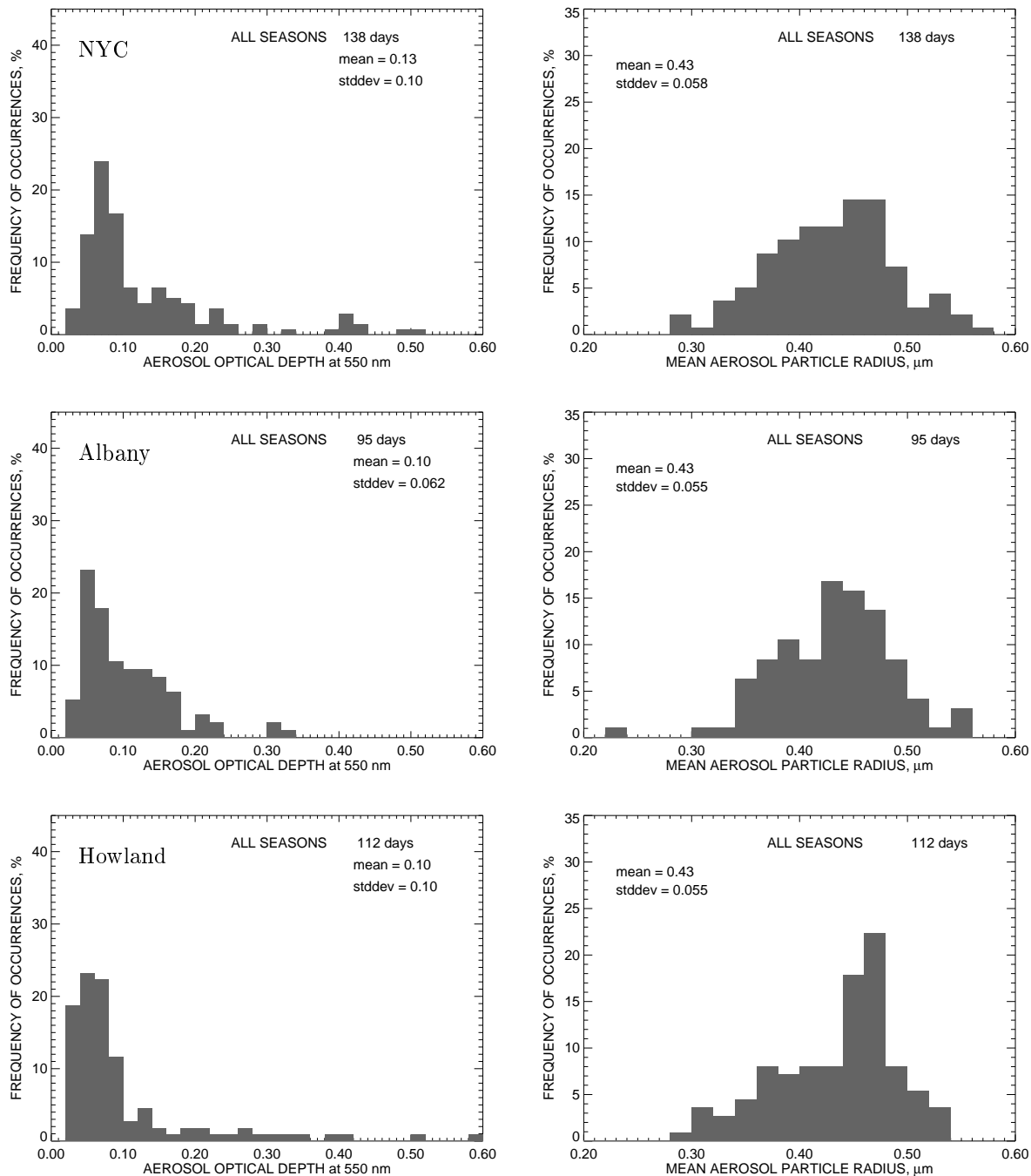
Figure 8.: Histograms for aerosol optical depth (at 550 nm) and mean particle size for three sites in the Northeastern US, periods of observations are the same as in Figs. 1, 2 and 3.
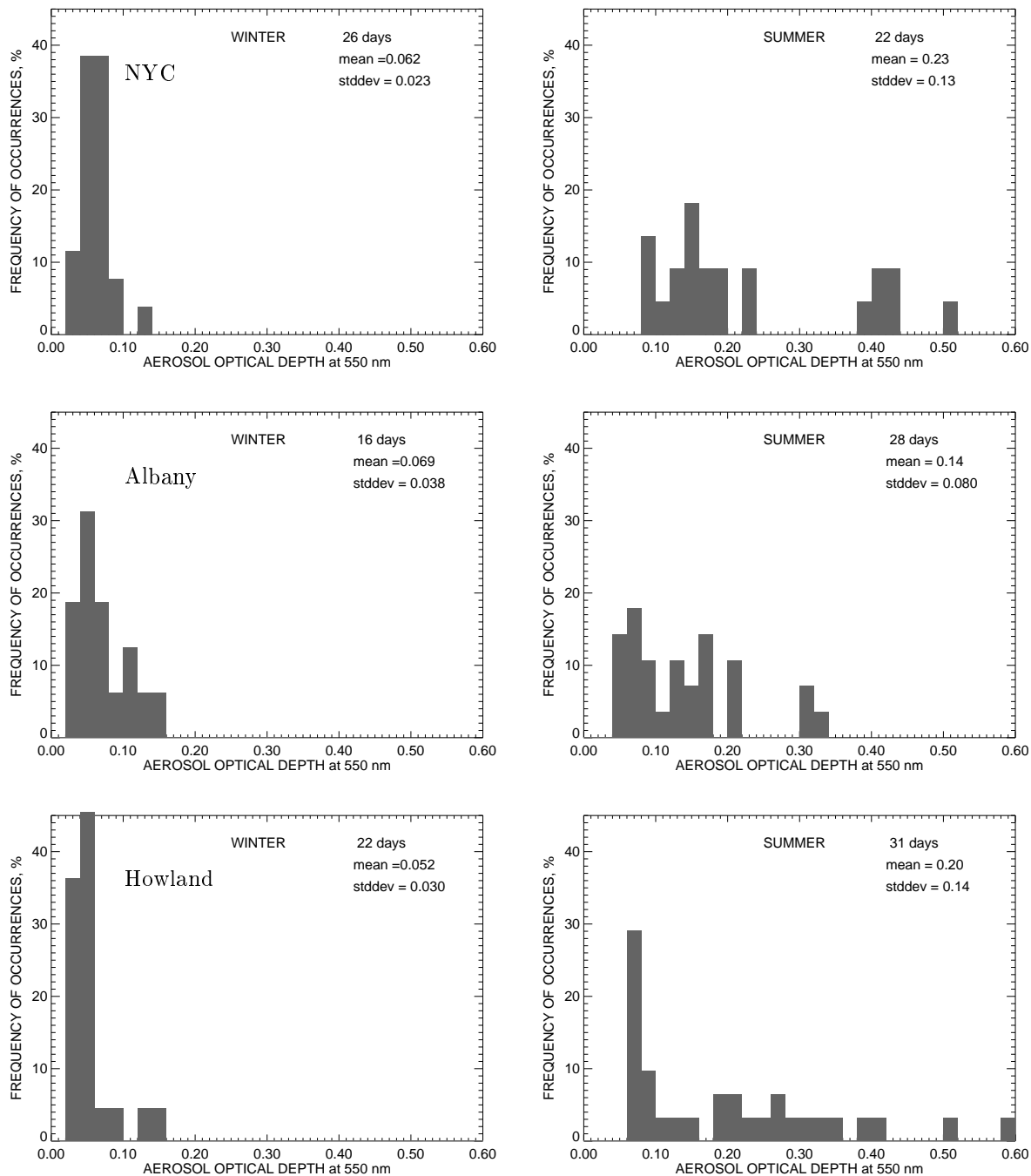
Figure 9.: Winter and summer histograms for aerosol optical depth (at 550 nm) for the same sites and periods as in Fig. 8.
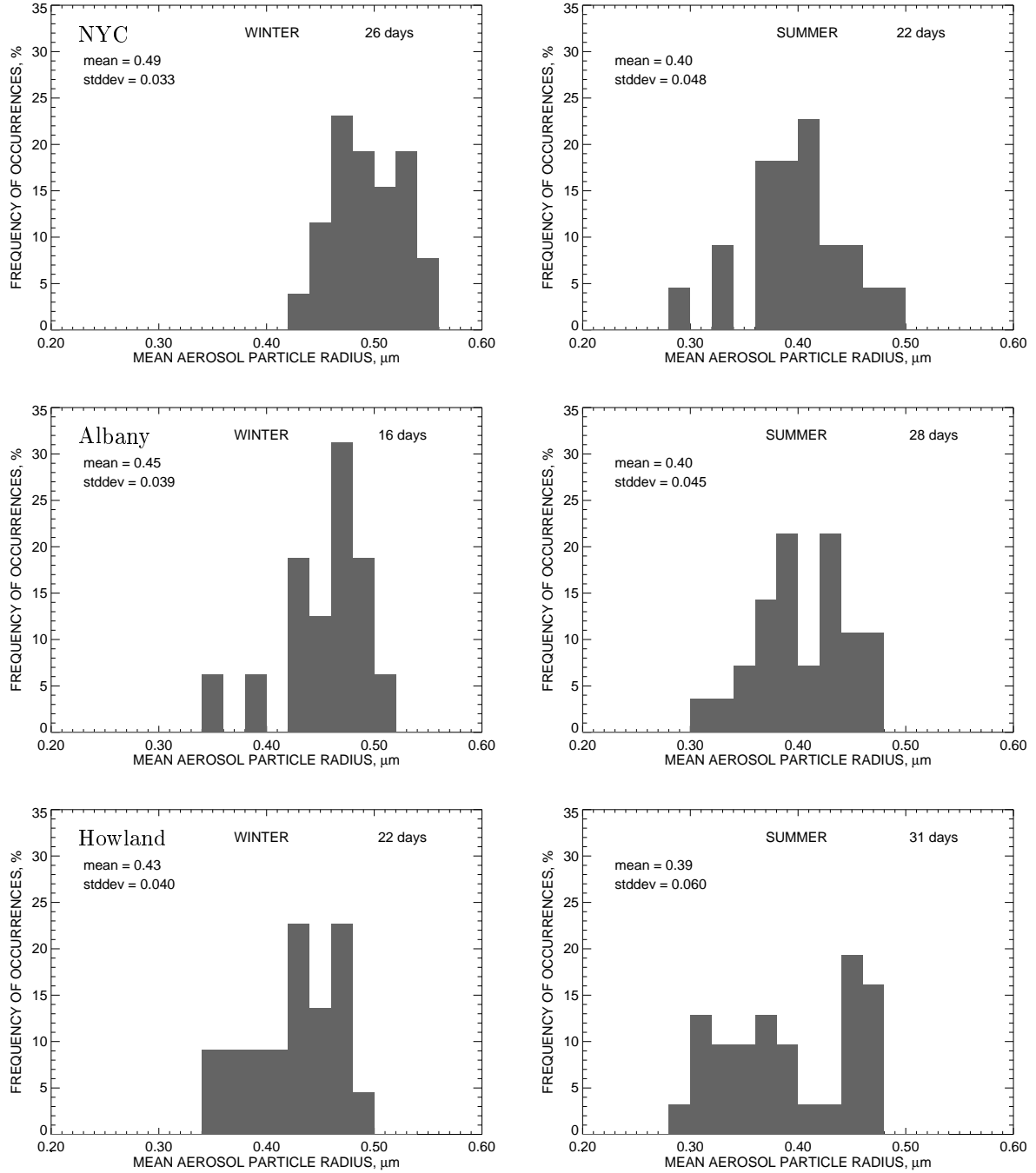
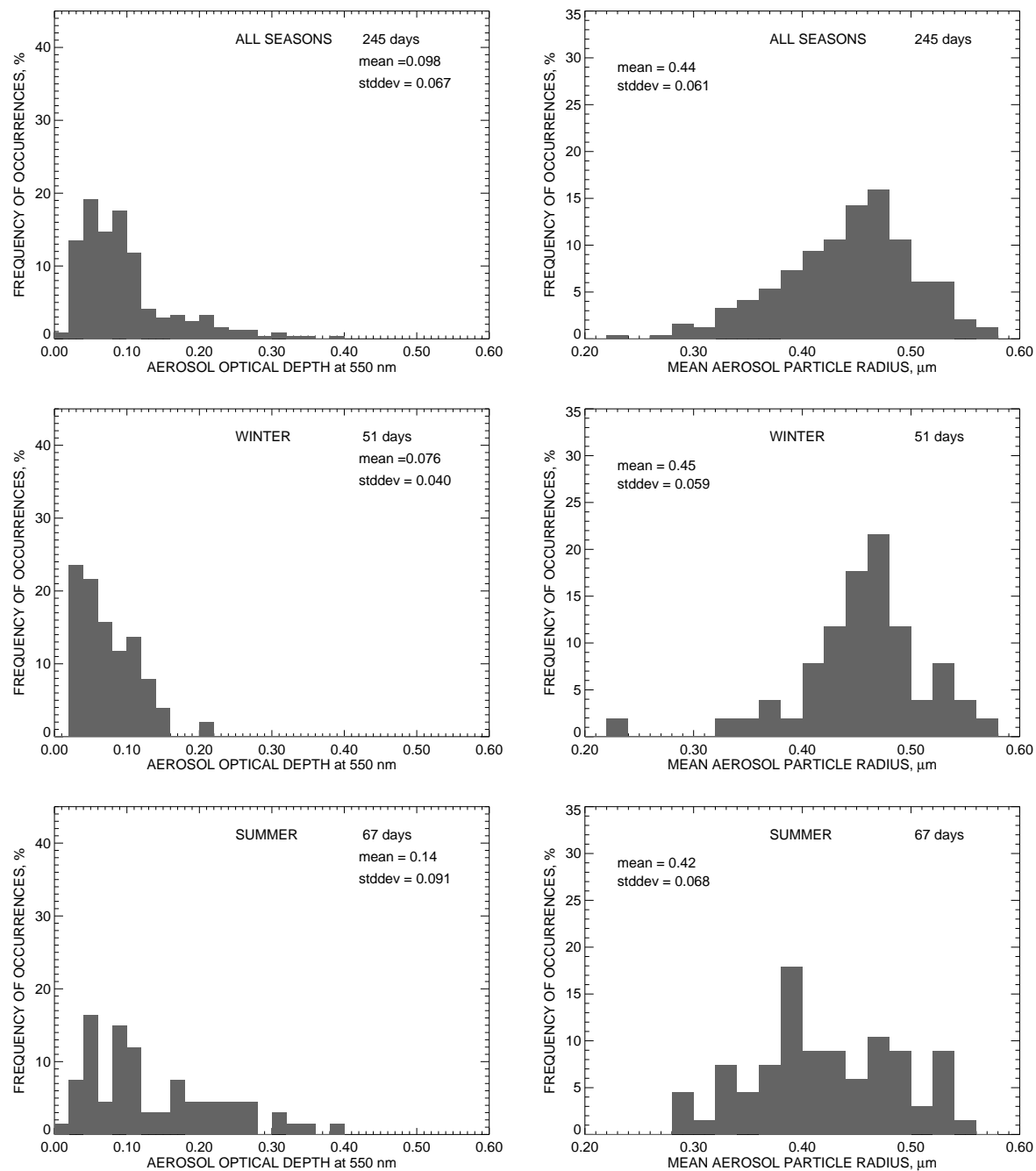**Figure 10.**: Same as in Fig. 9 but for mean column aerosol particle size.

Figure 11.: Histograms aerosol optical depth (at 550 nm) and mean column particle size for Albany, January 1995 - July 1997.
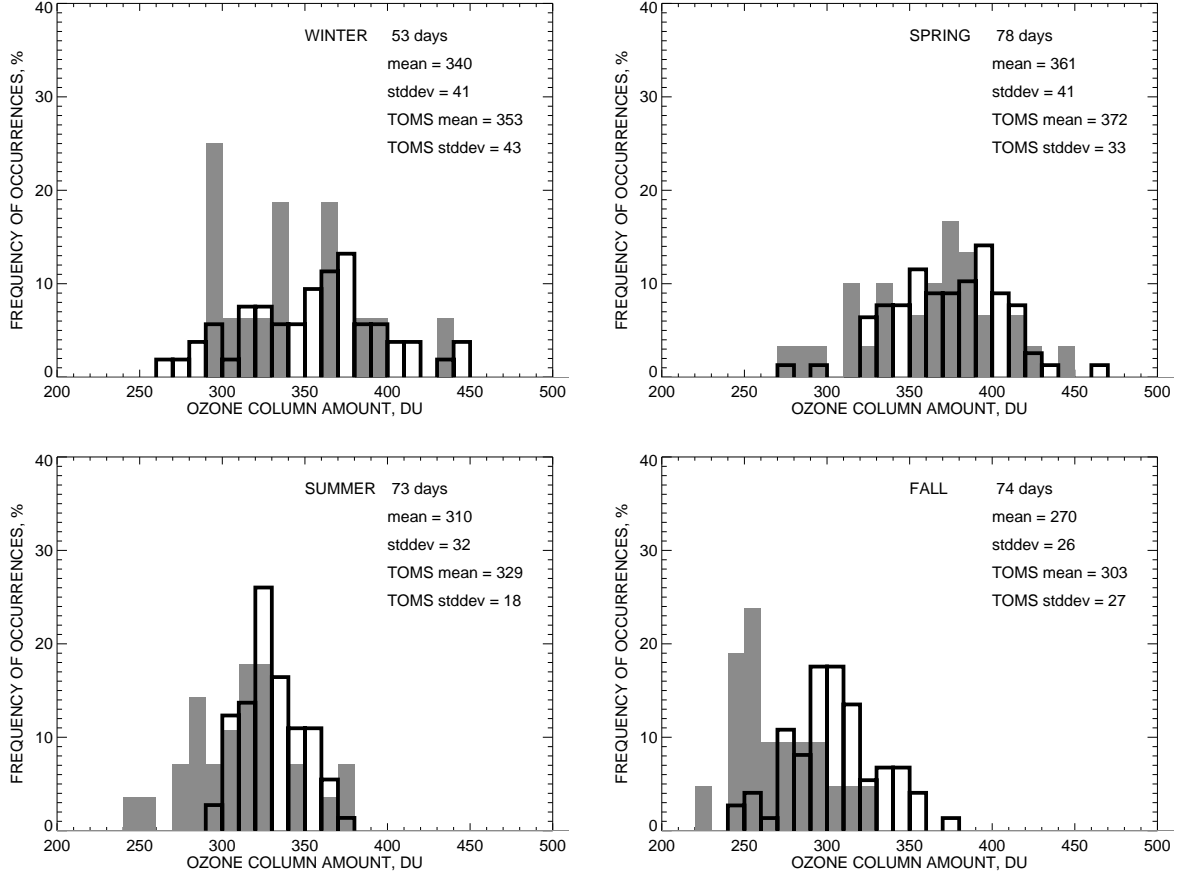
Figure 12.: Seasonal histograms for Albany, NY ozone column measured by MFRSR (shaded bins, data from 1996, 95 clear days) and by TOMS (clear bins, data from 1997, 278 days).

3.1. Northeastern United States

We present retrievals from data collected in New York City (SIRN) 9/95-11/96 (Fig. 1), Albany, New York (ASRC) 1-12/96 (Fig. 2), and Howland, Maine (ASRC) 1-12/95 (Fig. 3). Our retrieved aerosol properties, optical depth and effective radius for these sites are shown in Fig. 8. While differences exist in the shape of the frequency distributions, the mean values are similar at all three sites.

The area's climate is characterized by hot and humid summers and mild winters with strong northeastern winds. The mean temperature is (average of normal high and low temperature) 0^oC and 25^oC for January and July and the January and July average precipitation is 78 and 103 mm, respectively. For Albany, these values are -6^oC, 22^oC, 60 mm, and 81 mm for

January and July, respectively. While for Howland, the January and July values are -8^oC, 20^oC, 76 mm, and 84 mm, respectively for temperature and precipitation. As a measure of the relative changes in cloudiness, the Northeastern U.S. has about 150 sunshine hours/month in January and nearly 250 hours/month in July according to U.S. Geological Survey (1970).

As can be seen from our retrievals (Figs. 1-3), the seasonal variation in aerosol optical depth (i.e., summer/winter differences), as well as the mean summer values, are larger in the Eastern part of the U.S. than in the other regions of the country. For these Eastern sites, the larger aerosol optical depths in the summer are associated with smaller particle sizes which can be seen more clearly, in the histograms shown in Figs. 9 and 10. All three sites, exhibit similar behav-

14

ior, mean winter optical depths are 0.062, 0.069 and 0.052 increasing to 0.23, 0.14, 0.20 in the summer for New York City, Albany and Howland, respectively. Similarly, the mean aerosol radius is 0.49, 0.45, 0.43 in winter decreasing to 0.40, 0.40, and 0.39 μm for New York City, Albany and Howland, respectively in summer. (Note, that we can only retrieve the properties of the optically active aerosols while the sampling measurements (e.g., IMPROVE data) are mass concentrations that may be dominated by larger particles).
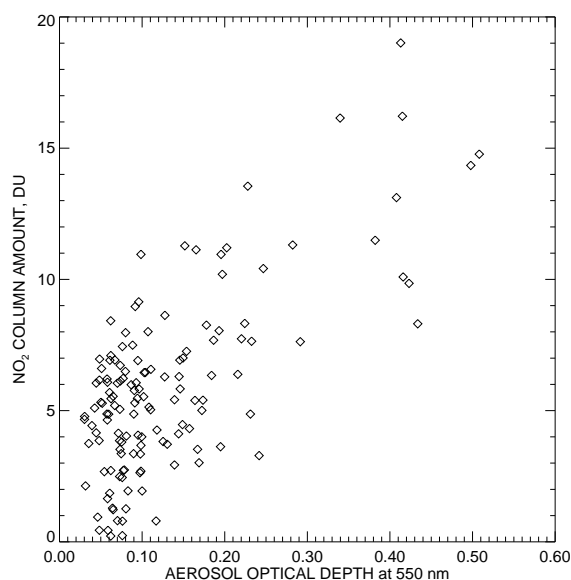

Figure 13.: Relationship between daily mean aerosol optical depths and NO$_2$ column amounts for NYC, period of observations is the same as in Fig. 1.

This seasonal behavior may be explained by enhanced summer production of secondary sulfate aerosols. The seasonal behavior of the sulfate aerosol is due mostly to the variations in OH and H$_2$O$_2$ concentrations that govern the oxidation of SO$_2$ to SO$_4^{-2}$. Thus, even if atmospheric chemistry models neglect the seasonal variation in SO$_2$ emissions they still achieve good agreement with the measurements (Chin et al. 1996). The seasonal change in particle size is also driven by seasonal changes in aerosol composition. During the summer, NOx photolysis leads to the production of tropospheric ozone, while the colder winter-time temperatures combined with the reduction in sunlight favors the production of nitrates. Thus, Malm et al.

(1994) find that the concentration of nitrates tends to be higher in the winter and spring than in summer and fall. Thus, the exact balance between aerosol production, transport and removal depends on location.

Nonetheless, it is interesting to note the similarity in the summer mean particle radii. The study by Schichtel (available on-line at http://capita.wustl.edu/ CAPITA/CapitaReports/PMFineAn) shows that the PM2.5 monitoring sites in the urban centers are dominated by local sources during the cold season (November - March), but that the Mid-Atlantic urban centers are dominated by regional sources during the warm season. Thus, it is likely that the similarity in aerosol properties at all three sites in summer reflects a regional source.

In order to evaluate how well we are capturing the annual cycle in aerosol properties and to investigate the effect that additional data would have on the shape of our optical depth and mean particle radius histograms, we analyzed a multi-year data set from Albany (Fig. 11). Comparison between the two sets of Albany histograms shows that with additional data the shape of the distribution begins to fill in. The width of the distribution also increases. For example, the mean winter mean particle radius changes from 0.45 μm (standard deviation of 0.039) to 0.45 μm (standard deviation of 0.059) going from the single year to the multi-year data set, respectively. While the mean summer mean particle radius changes from 0.4 μm (standard deviation of 0.045) to 0.42 μm (standard deviation of 0.068). Similarly, the optical depths show little variation between the single year and multi-year values. Based on this comparison, we believe that our analysis is adequately capturing the seasonal variation in aerosol properties. While differences in the shape of the histogram for Albany between the single-year and multi-year data records precludes drawing conclusions that are based on differences in the shape of the mean particle radius histogram, the data clearly indicate seasonal changes in aerosol properties including seasonal changes in aerosol size.

We note that our Eastern sites are relatively distant from industrial sulfate emissions sources (Benkovitz et al. 1996). Higher aerosol optical depths can be expected nearer to the sources (e.g. in Pennsylvania, Ohio or West Virginia), consistent with the MFRSR-derived optical depths available at the ASRC network website (http://hog.asrc.cestm.albany.edu/) and the location of the sulfate aerosol plume (Hogan and Rosmond 1991) modeled by the Naval Research
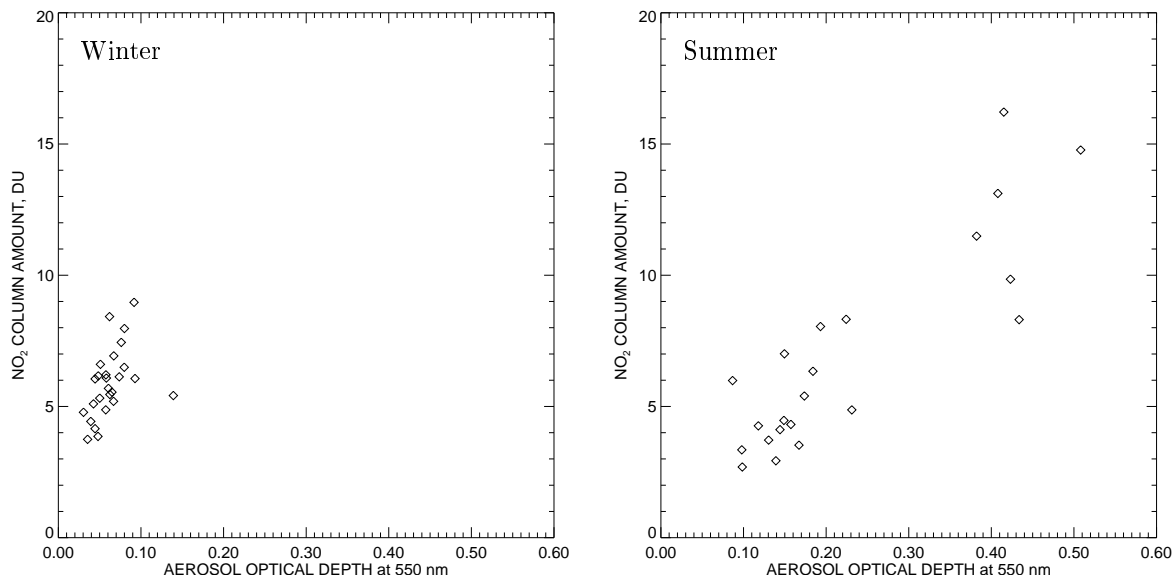
Figure 14.: Same as in 13 but separately for winter and summer.

Laboratory, Monterey (available on-line from http://www.nrlmry.navy.mil/aerosol/).

In Alexandrov et al. (2001), we compared the results of our ozone column retrievals with the TOMS measurements for both New York City and Albany. This revealed a greater positive bias between our results and TOMS measurements for Albany (29 DU) than for New York City (10 DU). To investigate whether we are adequately capturing the seasonal cycle of ozone, we compared our seasonal variability with that measured by TOMS. As shown in Fig. 12, in both data sets the ozone column amounts are more variable in winter and spring than summer and fall. The seasonal cycle retrieved here compares favorably with that retrieved by TOMS, column ozone peaks in spring and has a fall minimum. Moreover, since ozone is largely stratospheric, the variability in column ozone is comparable at all three sites.

The situation is quite different for NO_2. Here comparison of Figs. 1, 2 and 3 reveals that the NO_2 column amounts are larger in New York City and Albany than in Howland, which is consistent with spatial variations in the strength of the tropospheric source. Higher retrieved NO_2 column amounts are suggestive of pollution, so we examined the relationship between aerosol optical depth and NO_2 column. As can be seen in Fig. 13, there appears to be a rela-

tionship between NO_2 column amount and aerosol optical depth, particularly at larger optical depth. Because there are seasonal changes in both NO_2 and aerosol optical depth, the data are also separated by season. Fig. 14 shows that, for the most part, the winter-time NO_2 columns and aerosol optical depths vary independently, while in summer, the data are suggestive of a common source, with larger aerosol optical depths associated with larger NO_2 columns. Similar relationships are also found for Albany and Howland.

3.2. Southern Great Plains, Oklahoma

Results of our analysis of the Southern Great Plains, Oklahoma (ASRC and DOE ARM Program) data for 1994 (Fig. 4) are different from our eastern sites. The U.S. Southern Great Plains (SGP) Cloud and Radiation Testbed (CART) site is the field measurement site established by DOE's Atmospheric Radiation Measurement (ARM) Program. The site consists of *in situ* and remote-sensing instrument clusters arrayed across approximately 55,000 square miles (3×4 degrees) in north-central Oklahoma and south-central Kansas. The MFRSR data record at the SGP Central Facility starts in 1993.

The SGP site has mean January and July temperatures of 0^oC and 28^oC, respectively, while the
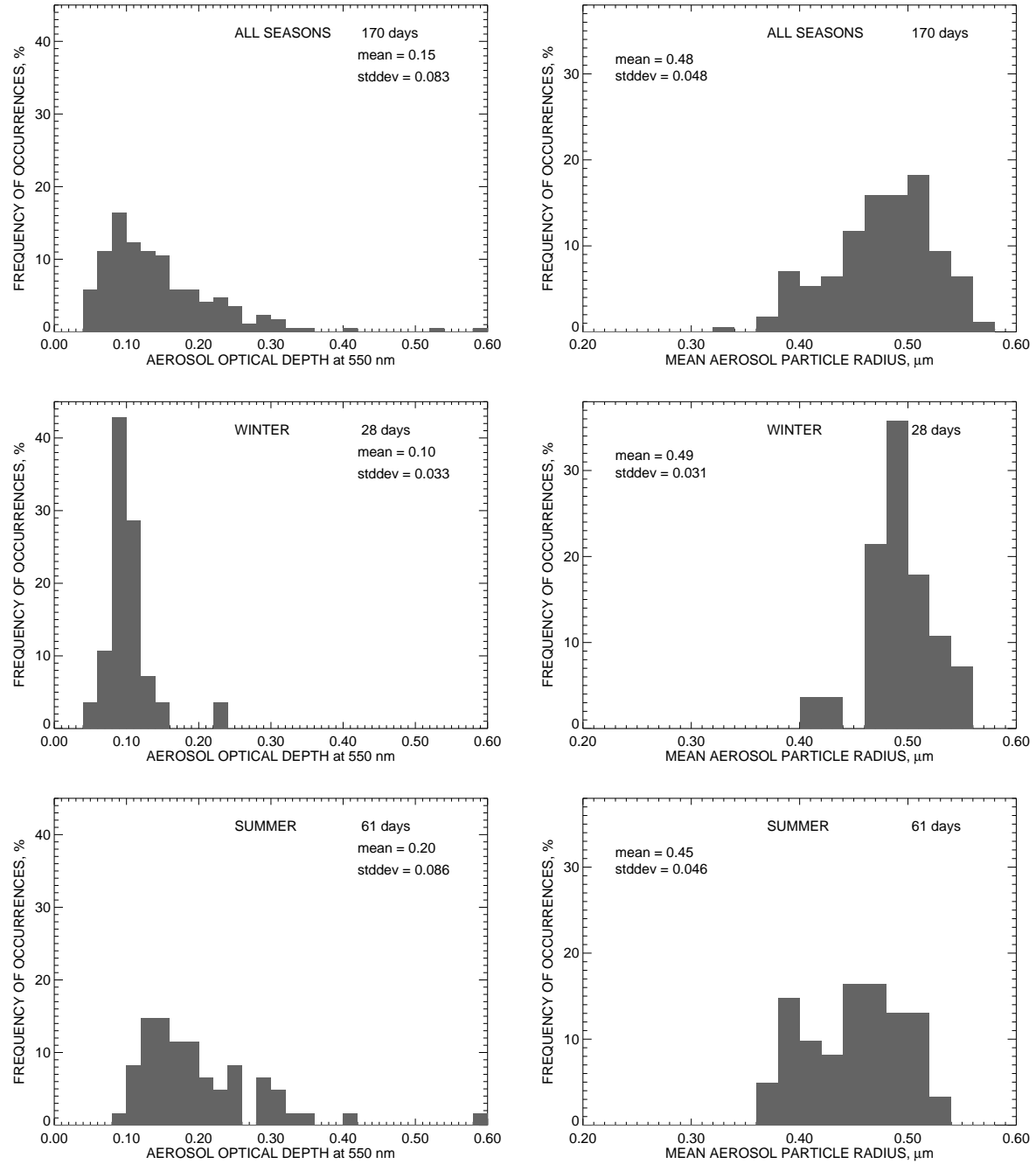
Figure 15.: Same as in Fig. 11 but for Southern Great Planes site, period of observations is the same as in Fig. 4.

January and July mean precipitation totals are 21 and 104 mm, respectively. Monthly sunshine in Oklahoma is 200 hours in January and about 350 hours in July. This is larger than in the Northeastern U.S., explaining the larger number of data points in Fig. 4 compared with for example, Fig. 1.
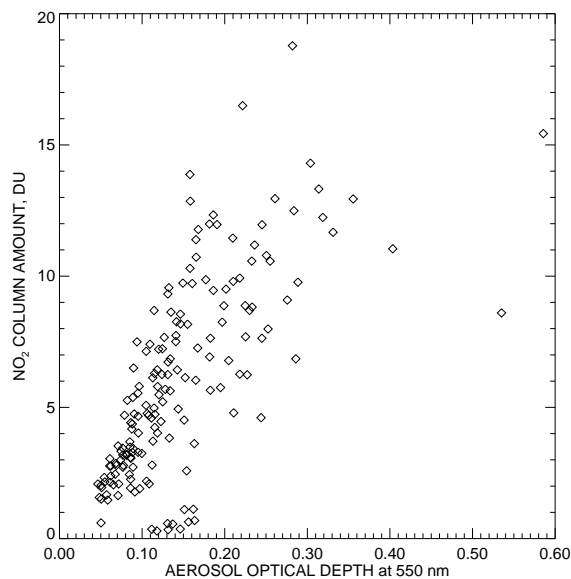

Figure 16.: Same as in Fig. 13, but for Southern Great Planes site, period of observations is the same as in Fig. 4.

Aerosols at this site come from both local and remote sources including agricultural activities, transport of pollution from industrial areas, Central America's fire smoke (Peppler et al. 2000), and even Sahara dust (Perry et al. 1997). Histograms of the aerosol properties, Fig. 15, show that the mean aerosol optical depth doubles from 0.1 in winter to 0.2 in summer. In addition, the width of the optical depth distribution increases. As is the case for our Eastern sites, the mean aerosol mean particle size decreases from winter to summer, and there is reason to believe that the seasonal cycle of aerosol similarly reflects the influence of sulfate aerosols.

The relatively high NO_2 amounts retrieved at the SGP site combined with the seasonal dependence are suggestive of the transport of polluted air masses from Texas by seasonal flows that are especially strong in summer time (U.S. Geological Survey, 1970). Figure 16 suggests that there is a relationship between NO_2

column amounts and aerosol optical depth in the annual data. As is the case for our Eastern sites, the strength of the relation is strongest in summer (Fig. 17). The relatively short lifetime of tropospheric NO_2 (roughly 24 hours) compared with that of aerosol provides limits on the distance from the source of the tropospheric pollution. We note that the SGP site is also located near local NO_2 emissions sources (cf., EPA data at http://www.epa.gov/airs/rvpltno2.gif).

3.3. Central Plains, Colorado

The Central Plains Experimental Range (CCPER) receives about 305 mm of precipitation per year (6.6 mm is January norm, 48.6 is normal for July), and is very dry compared to most of the other sites. The mean January and July temperatures are -3°C and 21°C, respectively. Sunshine amounts are roughly 180 and 350 hours for January and July. CPER is located approximately 50 km North of Denver but is not typically in Denver's air shed. The site is frequently used as a background site for many measurements. Its chief anthropogenic aerosol sources are in Cheyenne, Wyoming some 40 km to the North, and they are not very strong.

For this site the retrieved values of AOD and aerosol size for January - June 1996 (Fig. 5) are in agreement with the site climatology. The aerosol optical depth values are very low with summer maximum of about 0.1 and winter minimum of approximately 0.03. The retrieved NO_2 column values are also very small, further indicating that this site is not appreciably affected by tropospheric pollution.

3.4. Davis, California

As an example of a western site, we consider the data from the USDA site in Davis, California (Fig. 6) for the year 1996. Davis is surrounded by open space that includes some of the most productive agricultural land in the state. Sacramento is 15 miles to the east, and San Francisco is 72 miles to the southwest. Winters in Davis are generally mild (mean January temperature is 7.5^{o}C). While it rarely snows, it often rains (106 mm of precipitation is normal for January, with only about 150 hours of sunshine). Summers are sunny (with almost no clouds during the whole season, with about 420 hours of sunshine is typical for July). The mean July temperature is 24°C and conditions are very dry, averaging only 0-1.3 mm of precipitation in July. A reliable sea breeze usually cools overnight temperatures.
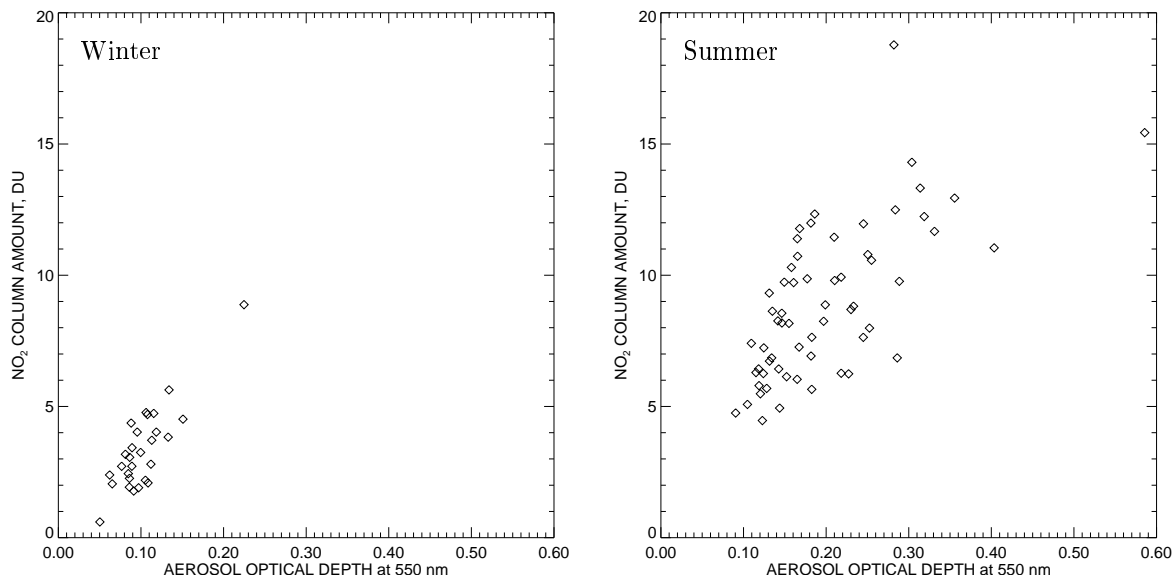
18

Figure 17.: Same as in 16 but separately for winter and summer.

Aerosols in the area consist of sulfates, nitrate, soil dust, organic carbon, and sea salt. While aerosol optical depth has a strong seasonal cycle, the maximum is shifted to the spring suggesting that agricultural activities are contributing to the increase in aerosol load at this site. Histograms of aerosol properties (Fig. 18) exhibit the same pattern as found at other sites, smaller optical depths and larger particles in the winter changing to larger optical depths and smaller particles in the summer. Interestingly, while our retrieved NO_2 column amounts are smaller in Davis than in New York City, the relationship between NO_2 and aerosol optical depths suggests that pollution contributes to the aerosol load in all seasons (Figs. 19, 20).

3.5. Eugene, Oregon

Mild winters, long growing seasons, and few drastic weather changes are characteristic of Eugene, Oregon. Normal annual rainfall totals are highest in the wet period from September to June with 213 mm and 7 mm in January and June, respectively. The pronounced wet period, strongly affects the sampling of sunphotometer measurements with the number of hours of sunshine changing from 80 in January to almost 300 in July. The mean January and July temperatures are respectively $4.5^{o}C$ and $20^{o}C$. Western

winds from the Pacific Ocean dominate during the wet season. Aerosol sources include biomass burning from agricultural grass fields in the fall as well as industrial pollution transport from Willamette Valley and possibly from California Central Valley (Holben et al. 2000). Organic carbon aerosols constitute the main part of the fine aerosol mass (Malm and Sisler 2000).

MFRSR retrievals for a one year period from May, 1997 to May, 1998 for Eugene indicate that there are very few cloud-free measurements (or measurement periods) during the wet season (Fig. 7). In agreement with the AERONET measurements (Holben et al. 2000), we find that the background aerosol optical depth is low (less than 0.1) and does not exhibit a pronounced seasonal variability. Similarly, aerosol size shows little seasonal variability. High AOD values toward the end of April, 1998 correspond to a China dust transport event (the data for this particular period is also shown in Fig. 21). This dust transport event following an unusually intense dust storm in China on April 15, was described by Gueymard et al. (preprint available from http://solardat.uoregon.edu/PDF/China Dust Effects on US.PDF); it even has its own website (http://capita/wustl.edu/Asia-FarEast/).
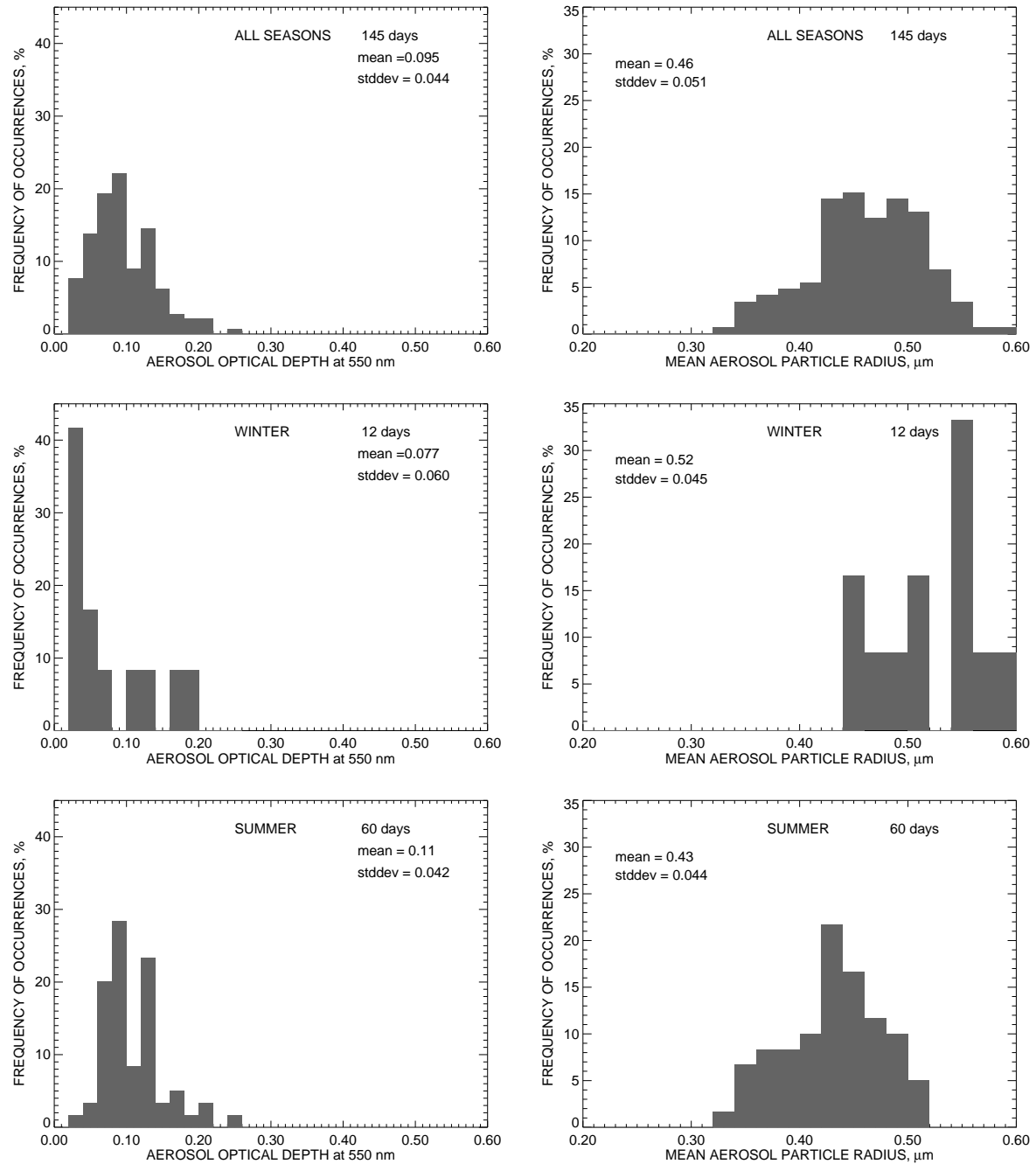Our retrievals indicate aerosol optical depths (at 550

Figure 18.: Same as in Fig. 11 but for Davis, California, period of observations is the same as in Fig. 6.

nm) of up to 0.4, and large particle sizes. As can be seen for this particular data subset, the presence of Asian dust results in a broad aerosol size distribution, and for the retrieved ozone and NO_2 columns (Fig. 21), sensible retrievals can only be obtained under the assumption of a large effective variance for the aerosol size distribution.
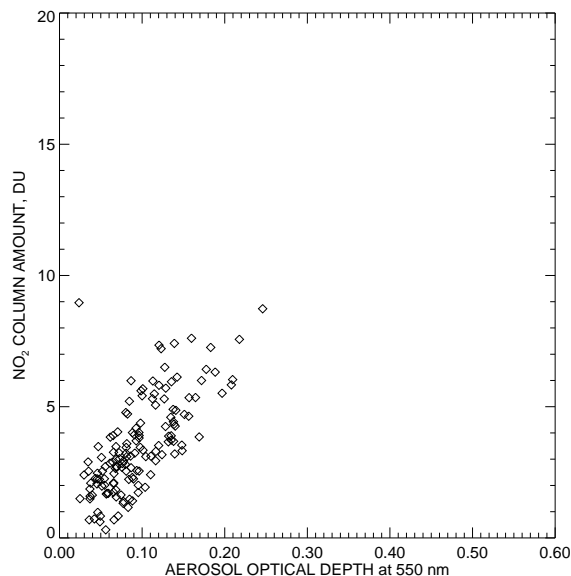

Figure 19.: Same as in Fig. 13, but for Davis, California, period of observations is the same as in Fig. 6.

3.6. Large-scale geographical variability

By combining our results from these sites, we can create a large-scale picture of aerosol seasonal and geographic behavior shown in Fig. 22. The sites and periods depicted are (from West to East): Eugene, Oregon (SIRN) 5/97-5/98; Davis, California (USDA) 1-12/96; Salt Lake City, Utah (SIRN) 2/97-1/99; Central Plains Experimental Range, Colorado (USDA) 1-6/96; Southern Great Plains, Oklahoma (ASRC and DOE ARM Program) 1-12/94; Miami, Florida (University of Miami) 5/94-5/95; New York City (SIRN) 12/95-11/96; Albany, New York (ASRC) 1-12/95; and Howland, Maine (ASRC) 1-12/95. To provide an indication of the geographic coverage possible with MFRSR data, we indicate the locations of a number of other MFRSR sites with dots. Geographic areas with multiple MFRSR instruments, such as the

Department of Energy's Atmospheric Radiation Measurement Programs extended facility which has 21 MFRSRs distributed over a 3×4° grid are represented by a single dot.

Seasonal means of aerosol optical thickness (at 550 nm wavelength) and effective radius of the aerosol size distribution (an effective variance of 0.2 is assumed for this plot) are shown for 9 sites by small histograms placed at the locations of the sites. The upper (black) bins depict mean optical thickness and the lower (white) bins represent the mean effective radius. Winter (December, January and February), spring (March, April and May), summer (June, July and August), and fall (September, October, and November) means are shown in the corresponding bins from left to right, respectively.

Based on our retrievals the summer/winter variations in aerosol optical thickness are larger in the Eastern part of the US than in other parts of the country. Interestingly, we find that aerosol optical depth histogram for the Southern Great Plains is shifted toward larger optical depths than on either coast. Clear days in this region are associated with higher aerosol optical depths. Seasonal changes in mean aerosol radius are similar at all of these sites. While the histograms of the retrieved mean aerosol radius are suggestive of characteristic differences between these sites, additional data analysis is required before these can be meaningfully interpreted. Nonetheless, the data indicate spatial differences in the aerosol properties. For example, the similarity of the retrieved aerosol properties during summer for our eastern sites is consistent with a regional aerosol source while the winter data are consistent with local sources.

Figure 23 shows the seasonal behavior of NO_2 (upper bins) and ozone (lower bins) for these sites. The column amounts less than 1 DU are not shown, the NO_2 at such sites is predominantly stratospheric. At all other sites, we find an appreciable tropospheric component.

The retrieved ozone column amount has a spring maximum in agreement with the expected seasonal change for the locations considered. While for the NO_2 column amount the maximum usually occurs in summer and is most likely a photochemical effect. The correlation between NO_2 column amounts and aerosol optical depth suggests that both share a common pollution origin. The association of the increased NO_2 with tropospheric pollution is further supported by the correspondence of the geographic pattern detected here. We find that the largest NO_2 column
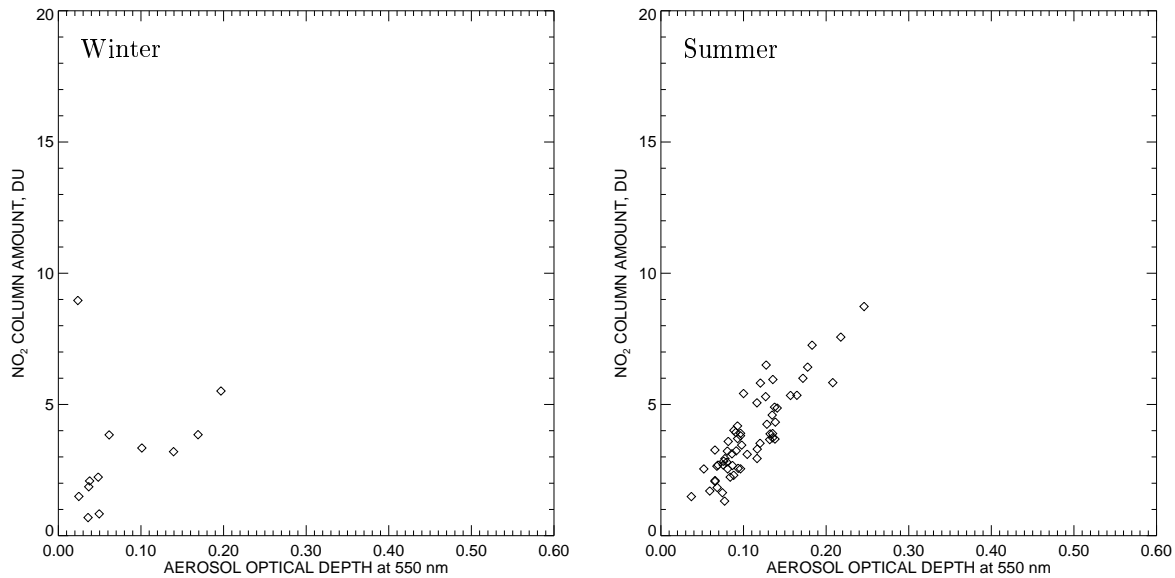
Figure 20.: Same as in 19 but separately for winter and summer.

amounts occur in the North-Eastern portion of the United States consistent with the spatial pattern of nitrogen oxide emissions (Logan 1983; Benkovitz et al. 1996). Similarly, this spatial pattern is in excellent agreement with the GOME maps of the tropospheric residual (Leue et al. 2001), except that our retrieved NO_2 column amounts are significantly larger than those inferred from the GOME measurements. As discussed in Richter and Burrows (2001), the GOME measurements are a lower limit on the amount of tropospheric NO_2.

Since the stratospheric amount of NO_2 is much smaller than that of ozone, we are able to detect the tropospheric NO_2 enhancement, whereas for ozone, the tropospheric enhancement is lost in the noise of the measurement (e.g., comparable to the bias or standard deviation in the comparison with TOMS). Thus while ozone and NO_2 pollution-related emissions are of a similar magnitude (see e.g. New York State Department of Environmental Conservation, http://www.dec.state.ny.us), the relative contribution of the boundary layer component to the total column optical thickness is substantially larger for nitrogen dioxide than for ozone. We believe this accounts for our higher NO_2 column amounts compared to GOME satellite retrievals (Burrows et al. 1999), while our ground-based ozone column values are in

good agreement with TOMS measurements (TOMS, http://toms.gsfc.nasa.gov). As discussed in Alexandrov et al. (2001), further support for our retrieved NO_2 column amounts comes from the analysis of co-located differential absorption spectrometer and sunphotometer measurements for a suburban site in Ontario by Schroeder and Davies (1987). They found that NO_2 column amounts ranged from 0.04 to 12.6 DU with a median of 1.7 DU, and within the range of other published values (Noxon 1978, Pujadas et al. 2000).

4. Discussion

We have adopted a different strategy for the analysis of MFRSR measurements compared with earlier retrievals. In our approach, we rely solely on the information content of the MFRSR measurements to self-consistently and simultaneously retrieve times series of aerosol properties (AOD and effective radius), column amounts of ozone and NO_2 along with the instrument's calibration. The details of our retrieval/calibration algorithm for MFRSR data analysis and validation of our retrieved quantities through comparisons with other measurements are presented in Alexandrov et al. (2001). In this paper, we have presented our results for multiple U.S. sites to fur-
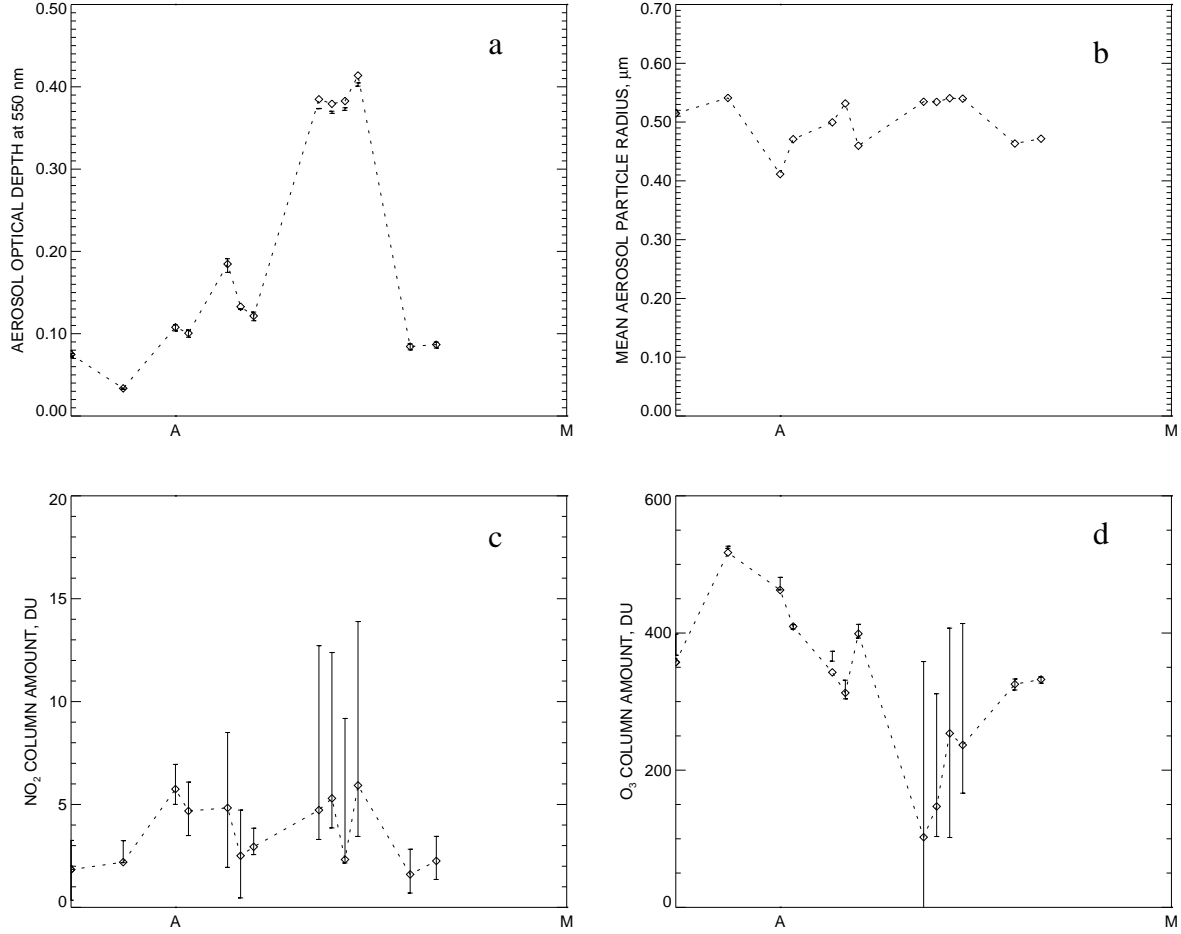
Figure 21.: China dust transport event in Eugene, Oregon in April, 1998. Upper ends of error bars in the NO_2 plot and lower ends of error bars in the O_3 plot correspond to the minimal assumed aerosol $v_{eff} = 0$.

ther test our retrieval algorithm and to investigate the type of information that MFRSR measurements can contribute to a ground-based aerosol climatology. In our analysis we are using the MFRSR filters nominally located at 415, 500 610, 670 and 870 nm to retrieve time series of aerosol optical depth and column mean particle size, as well as ozone and nitrogen dioxide column amounts. The MFRSR has an additional channel at 940 nm that can be used to retrieve column water vapor. However, analysis of this channel requires a different calibration approach and is not included in this paper. Unfortunately, it is not possible to uniquely constrain the width of the aerosol size distribution using the nominal MFRSR filters because

of trade-offs exist between small particle extinction and NO_2 absorption in the shortest filters. Due to this ambiguity, we present our results for a range of aerosol size distributions, which are specified by the variance of the size distribution. We use the results at the smallest and largest variances to express the uncertainties entailed in our retrieved quantities.

Despite these uncertainties, our results clearly show that column amounts of NO_2 vary with time and location. Moreover, our retrieved NO_2 columns are larger than those retrieved from the GOME measurements for reasons described in Richter and Burrows (2001) and Leue et al. (2001), but consistent with other ground-based measurements (e.g., Schroeder et
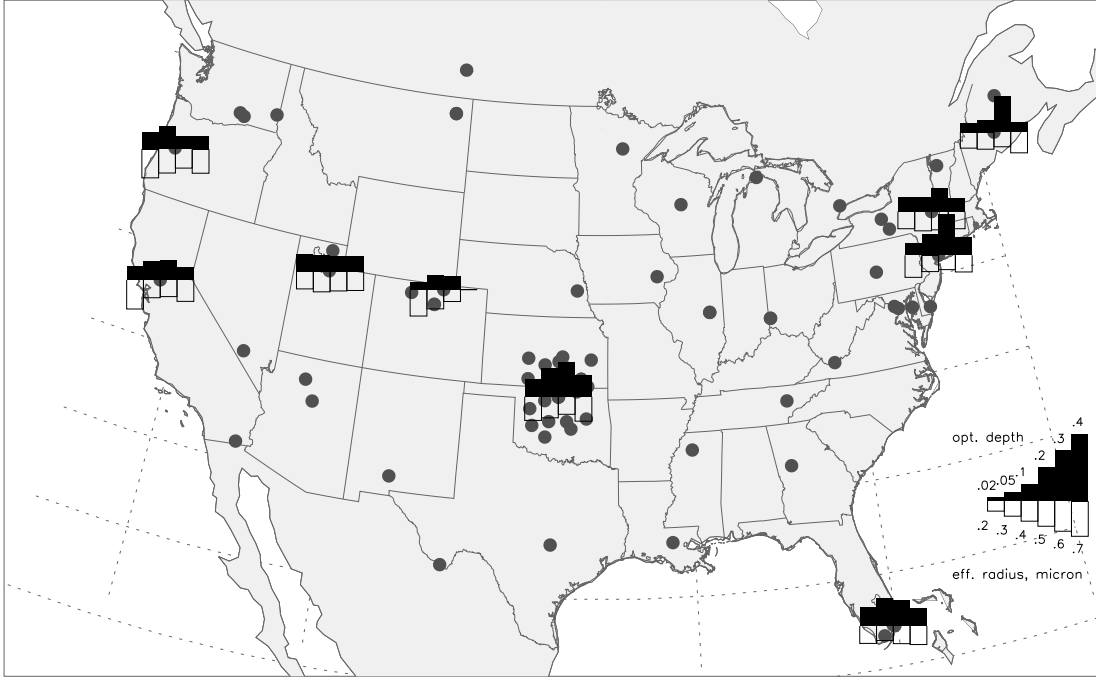
Figure 22.: Sample of seasonal behavior of aerosol optical depth at 550 nm (upper bins) and effective radius of the aerosol size distribution (lower bins) for 9 sites in the continental US. Winter, spring, summer and autumn means are represented by the corresponding bins from left to right. Note that the histogram for Eugene, Oregon is affected by the China dust transport event in spring, 1998. Fall measurements at CPER were not included into analysis. To show the geographic coverage of MFRSR measurements the locations of instruments belonging to the ASRC, SIRN, SURFNET, and USDA UVB networks are depicted by dark dots.

al. 1987, Noxon 1978, Pujadas et al 2000). Thus, we agree with (Richter and Burrows, 2001) that the GOME values represent a lower limit to the amount of tropospheric NO_2. A discussion of the source of errors in the GOME retrieval can be found in Leue et al. (2001) and Richter and Burrows (2001) and include errors in the specification of the surface albedo, the effects of sub-pixel clouds (the amount of NO_2 is found to be inversely correlated with cloud fraction), and errors in the calculation of the air mass factor which contribute to the underestimation. Nonetheless, the spatial and seasonal pattern of our retrieved results is in qualitative agreement with the GOME measurements.

Our NO_2 column amounts combined with the more complete spatial pattern of NO_2 variability provided by the GOME measurements, have profound impli-

cations for aerosol climatologies and other retrievals that are made without regard for NO_2 absorption. For example, Schroeder and Davies (1987) analyzed the effect that neglect of NO_2 absorption would have on the aerosol retrievals. As suggested by Shaw (1976), they found that significant errors in aerosol optical depth arise from the neglect of NO_2 absorption. Moreover, the magnitude of the error depends on the column amount of NO_2 present. Thus, they found that the aerosol optical depths were reduced by 22-47%, 12-25%, 3-6% and 1% at wavelengths of 400, 500, 610, and 670 nm, respectively, for NO_2 column amounts of 3 and 6 DU, respectively.

More importantly, Schroeder and Davies (1987) investigated the minimum (threshold) NO_2 amount required to significantly affect aerosol optical depth distributions in the statistical sense of using a Kolmogorov-
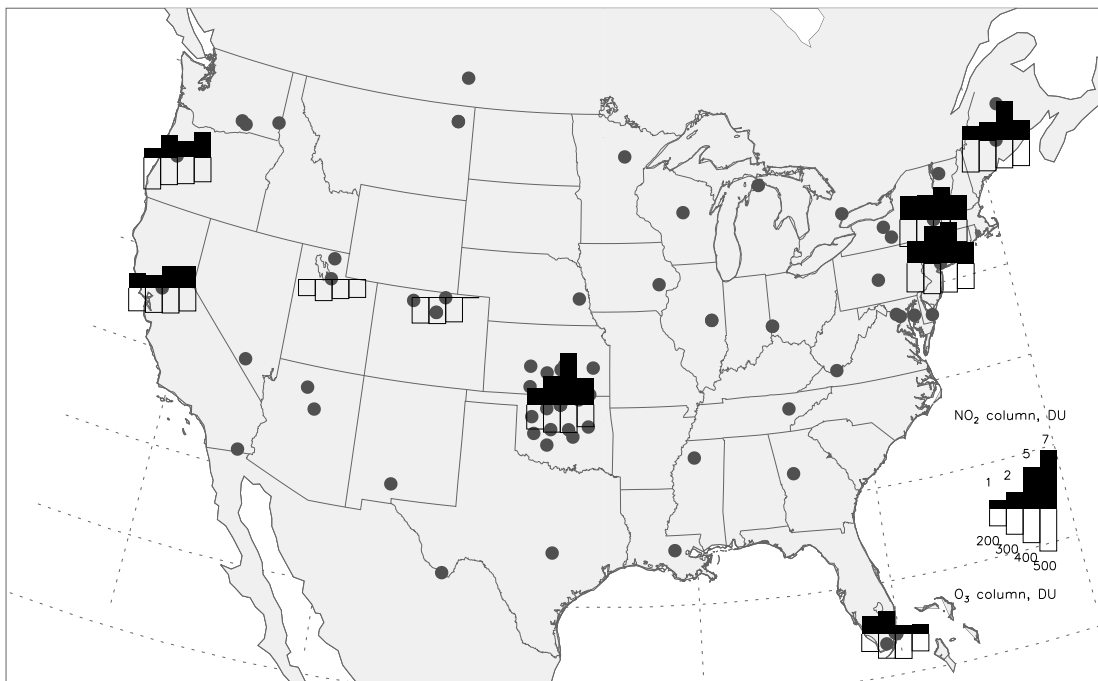
Figure 23.: Same as in Fig. 22 but for seasonal behavior of NO_2 (upper bins) and ozone (lower bins) column amounts. NO_2 amounts less than 1 DU are not shown (CPER and Salt Lake City cites).

Smirnov test to determine statistical significance at the 95% confidence interval. At 400 nm, the threshold was found to be 1.3 DU, an amount that was exceeded by 66% of their suburban measurements while at 500 nm the threshold was found to be 1.4 DU, an amount exceeded by 62% of their measurements. Thus, at their suburban site, NO_2 absorption reduced aerosol optical depths at shorter wavelengths in more than half of their observations. More importantly, Schroeder and Davies (1987) went on to examine the effect that neglect of NO_2 absorption would have on the inferred aerosol size distributions. In their analysis they used a Junge aerosol size distribution (Shaw et al. 1973). By comparing the exponent of the Junge aerosol size distribution retrieved with and without including NO_2 absorption they found that the difference in the two frequency distributions is statistically significant for column NO_2 amounts exceeding 0.6 DU, a condition that was met by 92% of their suburban measurements.

Including NO_2 absorption reduces the ratio of large

to small particles. Since we are retrieving gas column amounts along with the aerosol properties, we cannot uniquely invert our data to retrieve aerosol size distribution without their implicit tradeoff on gas column amount. However, since Schroeder and Davies (1987) used co-located differential absorption spectrometer measurements to retrieve the NO_2 column they could invert their sunphotometer measurements to retrieve the aerosol size distribution. Using King's (1978) constrained linear inversion method assuming a complex refractive index of 1.5 - $0.001i$ and equal experimental errors for all optical depths, they found that accounting for NO_2 absorption reduced the number of particles at radii smaller than 0.2 μm and at radii larger than 0.5 μm and for high NO_2 amounts, the bi-modal distribution inverted neglecting NO_2 absorption is replaced with a narrower uni-modal distribution when the retrieved optical depths are corrected for NO_2 absorption.

Since GOME measurements show that elevated tropospheric NO_2 values are associated with urban ar-

eas and regions of biomass burning, and since we find relatively large NO$_2$ columns at most of our sites (i.e., values in excess of the 0.6 DU required to significantly affect the retrieval of the aerosol size distribution, and frequently in excess of the 1.3 - 1.4 DU required to significantly affect the distribution of retrieved spectral optical depths as determined by Schroeder and Davies, 1987), it is therefore likely that aerosol optical depth climatologies constructed without regard for NO$_2$ absorption are probably overestimated by an amount that depends on the NO$_2$ concentration. Similarly, in biomass burning areas neglecting NO$_2$ would lead to systematic errors in the retrieved aerosol properties.

Our analysis indicates that MFRSR measurements can significantly contribute to ground-based aerosol climatologies. Due to the importance of NO$_2$, additional research is required to further validate our NO$_2$ columns and to explore ways to uniquely separate the competing contributions of small particle aerosol extinction and NO$_2$ absorption (e.g., through a change in the nominal filter set to include a filter at wavelengths shorter than 415 nm). Analysis of additional MFRSR measurements will fill in the spatial pattern of aerosol variability. Additional analysis and the inclusion of multi-year data records will provide a better description of the seasonal changes in the characteristic aerosol properties at each site (i.e., will allow us to separate transport events and extreme events from the base-line seasonal behavior).

References

Alexandrov, M., A. Lacis, B. Carlson, and B. Cairns, 1997: Retrieval of aerosol optical depth, aerosol size distribution parameters, ozone and nitrogen dioxide amounts from MFRSR data, *Proc. 7th Annual Atmospheric Radiation Measurement (ARM) Program Science Team Meeting*, San Antonio, TX, 379-383.

Alexandrov, M., A. Lacis, B. Carlson, and B. Cairns, 1999a: Validation of MFRSR data analysis: Comparison with the Langley approach, *Proc. 9th Annual Atmospheric Radiation Measurement (ARM) Program Science Team Meeting*, San Antonio, TX. [Available on-line from http://www.arm.gov/docs/documents/technical/ conf_9903.]

Alexandrov, M., A. Lacis, B. Carlson, and B. Cairns, 1999b: Atmospheric aerosol remote sensing by means of multi-filter rotating shadow-band radiometer, *J. Aerosol Sci.*, **30**, S615-S616.

Alexandrov, M., A. Lacis, B. Carlson, and B. Cairns, 1999c: Remote sensing of atmospheric aerosols, nitrogen dioxide and ozone by means of multi-filter rotating shadow-band radiometer, *Remote Sensing of Clouds and Atmosphere IV*, Proceedings of SPIE, Vol. 3867, 156-170.

Alexandrov, M., A. Lacis, B. Carlson, and B. Cairns, 2000: MFRSR-based climatologies of atmospheric aerosols, trace gases and water vapor, *Remote Sensing of Clouds and Atmosphere V*, Proceedings of SPIE, Vol. 4168, 9 pp., *in print*.

Alexandrov, M., A. Lacis, B. Carlson, and B. Cairns, 2001: Remote sensing of atmospheric aerosols and trace gases by means of Multi-Filter Rotating Shadowband Radiometer. Part I: Retrieval algorithm, *this issue*.

Benkovitz, C. M., T. Scholtz, L. Pacyna, L. Tarrson, J. Dignon, E. Voldner, P. A. Spiro, and T. E. Graedel, 1996: Global gridded inventories of anthropogenic emissions of sulphur and nitrogen, *J. Geophys. Res.*, **101**, 29239-29253.

Bigelow, D. S., J. R. Slusser, A. F. Beaubien and J. H. Gibson, 1998: The USDA Ultraviolet Radiation Monitoring Program, *Bull. Amer. Meteorol. Soc.*, **79**, 601-615.

Burrows, J. P., M. Weber, M. Buchwitz, V. Rozanov, A. Ladstatter-Weissenmayer, A. Richter, R. DeBeek, R. Hoogen, K. Bramstedt, K. U. Eichmann, and M. Eisinger, 1999: The global ozone monitoring experiment (GOME): Mission concept and first scientific results, *J. Atmos. Sci.*, **56**, 151-175.

Chin, M., D. J. Jacob, G. M. Gardner, M. S. Foreman-Fowler, P. A. Spiro, and D. L. Savoie, 1996: A global three-dimensional model of tropospheric sulfate, *J. Geophys. Res.*, **101**, 18667-18690.

Hansen, J. E., and L. D. Travis, 1974: Light scattering in planetary atmospheres, *Space Sci. Rev.*, **16**, 527-610.

Harrison, L. and J. Michalsky, 1994: Objective algorithms for the retrieval of optical depths from ground-based measurements, *Appl. Opt.*, **33**, 5126-5132.

Harrison, L., J. Michalsky, and J. Berndt, 1994: Automated multifilter shadow-band radiometer: instrument for optical depth and radiation measurement, *Appl. Opt.*, **33**, 5118-5125.

Herman, B. M., R. S. Browning, and J. J. De Luisi, 1975: Determination of the effective imaginary term of the complex refractive index of atmospheric dust by remote sensing: the diffuse-direct radiation method, *J. Atmos.*

Sci., *32*, 918-925.

Hogan, T. F., and T. E. Rosmond, 1991: The description of the Navy operational global atmospheri prediction system's spectral forecast model, *Mon. Wea. Rev.*, **119**, 1786-1815.

Holben, B.N., D. Tanre, A. Smirnov, T. F. Eck, I. Slutsker, N. Abuhassan, W. W. Newcomb, J. Schafer, B. Chatenet, F. Lavenue, Y. J. Kaufman, J. Vande Castle, A. Setzer, B. Markham, D. Clark, R. Frouin, R. Halthore, A. Karnieli, N. T. O'Neill, C. Pietras, R. T. Pinker, K. Voss, and G. Zibordi, 2000: An emerging ground-based aerosol climatology: Aerosol Optical Depth from AERONET, *submitted to J. Geophys. Res.*.

King, M. D., D. M. Byrne, B. M. Herman, and J. A. Reagan, 1978: Aerosol size distributions obtained by inversion of spectral optical depth measurements, *J. Atmos. Sci.*, **35**, 2153-2167.

Lacis, A. A., B. E. Carlson, and B. Cairns, 1996: Multi-Spectral Atmospheric Column Extinction Analysis of Multi-Filter Rotating Shadowband Radiometer Measurements, *Proc. 6th Atmospheric Radiation Measurement (ARM) Science Team Meeting*, San Antonio, TX, 145-148.

Leue, C., M. Wenig, T. Wagner, O. Klimm, U. Platt, and B. Jähne, 2001: Quantitative analysis of NO_x emissions from Global Ozone Monitoring Experiment satellite image sequences, *J. Geophys. Res.*, **106**, 5493-5505.

Logan, J. A., 1983: Nitrogen oxides in the troposphere: global and regional budgets, *J. Geophys. Res.*, **88**, 10785-10807.

Malm, W. C. and J. F. Sisler, 2000: Spatial patterns of major aerosol species and selected heavy metals in the United States, *Fuel Processing Technology*, **65-66**, 473-501.

Malm, W. C., J. F. Sisler, D. Huffman, R. A. Eldred, T. A. Cahill, 1994: Spatial and seasonal trends in particle concentration and optical extinction in the United States, *J. Geophys. Res.*, **99**, 1347-1370.

Noxon, J. F., 1978: Tropospheric NO_2, *J. Geophys. Res.*, **83**, 3051-3057.

O'Neill, N. T., A. Royer, and J. R. Miller, 1989: Aerosol optical depth determination from ground based irradiance ratios, *Appl. Opt.*, **28**, 3092-3098.

Peppler R. A., C. P. Bahrmann, J. C. Barnard, J. R. Campbell, M. D. Cheng, R. A. Ferrare, R. N. Halthore, L. A. Heilman, D. L. Hlavka, N. S. Laulainen, C. J. Lin, J. A. Ogren, M. R. Poellot, L. A. Remer, K. Sassen, J. D. Spinhirne, M. E. Splitt, and D. D. Turner, 2000: ARM Southern Great Plains site observations of the smoke pall associated with the 1998 Central American fires, *B. Am. Meteorol. Soc.*, **81**, 2563-2591.

Perry K. D., T. A. Cahill, R. A. Eldred, and D. D. Dutcher, T. E. Gill, 1997: Long-range transport of North African dust to the eastern United States, *J. Geophys. Res.*, **102**, 11225-11238.

M. Pujadas, J. Plaza, J. Terés, B. Artiñano, M. Millán, 2000: Passive remote sensing of nitrogen dioxide as a tool for tracking air pollution in urban areas: the Madrid urban plume, a case of study, *Atmos. Eviron.*, **34**, 3041-3056.

Richter, A. and J. P. Burrows, 2000: A multi wavelength approach to the retrieval of tropospheric NO_2 from GOME measurements, *Proc. ERS-ENVISAT Symposium*, Gothenburg, Sweden. [Available on-line from http://www.doas-bremen.de/paper/ esa_00_richter.pdf]

Richter, A. and J. P. Burrows, 2001: Tropospheric NO_2 from GOME measurements, *submitted to Adv. Space Res.*. [Available on-line from http://www.doas-bremen.de/paper/ COSPAR_2000_no2.pdf]

Schmid, B., J. Michalsky, R. Halthore, M. Beauharnois, L. Harrison, J. Livingston, P. Russel, B. Holben, T. Eck, and A. Smirnov, 1999: Comparison of aerosol optical depth from four solar radiometers during the Fall 1997 ARM Intensive Observation Period, *Geophys. Res. Lett.*, **26**, 2725-2728.

Schroeder, R. and J. A. Davies, 1987: Significance of nitrogen dioxide absorption in estimating aerosol optical depth and size distributions, *Atmos.-Ocean*, **25**, 107-114.

Shaw, G. E., 1976: Nitrogen dioxide – optical absorption in visible, *J. Geophys. Res.*, **81**, 5791-5792.

Tegen, I., P. Hollrig, M. Chin, I. Fung, D. Jacob, and J. Penner, 1997: Contribution of different aerosol species to the global aerosol extinction optical thickness: Estimates from model results, *J. Geophys. Res.*, **102**, 23895-23915.

U.S. Geological Survey, 1970: *The National Atlas of the United States of America*, U.S. Department of Interior Geological Survey, 417 pp.

M. D. Alexandrov, A. A. Lacis, B. E. Carlson, and B. Cairns, NASA Goddard Institute for Space Studies, 2880 Broadway, New York, NY 10025, Contact E-mail: `malexandrov@giss.nasa.gov`